

# UC San Diego

## UC San Diego Electronic Theses and Dissertations

### Title

Mechanisms of Regulation for Serine Protease Activity in the Rat Ileocecal Junction /

### Permalink

<https://escholarship.org/uc/item/3z22942v>

### Author

Tam, Derek Wai

### Publication Date

2014

Peer reviewed|Thesis/dissertation

UNIVERSITY OF CALIFORNIA, SAN DIEGO

**Mechanisms of Regulation for Serine Protease Activity in the Rat Ileocecal Junction**

A Thesis submitted in partial satisfaction of the Requirements for the degree Master of  
Science

in

Bioengineering

by

Derek Wai Tam

Committee in charge:

Professor Geert W. Schmid-Schönbein, Chair

Professor Michael J. Heller

Professor Erik Kistler

2014

Copyright

Derek Wai Tam, 2014

All rights reserved

The thesis of Derek Wai Tam is approved and it is acceptable in quality and form for publication on microfilm and electronically:

---

---

---

Chair

University of California, San Diego

2014

## **DEDICATION**

This thesis is dedicated to my parents, Clement Tam and Siu Tam, both of whom provide me constant love and support. Their encouragement of my dreams and goals allowed me to go as far as I did, and gave me the strength and due diligence needed in writing this thesis.

# TABLE OF CONTENTS

Signature page.....	iii
Dedication.....	iv
Table of Contents.....	v
List of Figures.....	vii
List of Tables.....	ix
Acknowledgments.....	x
Abstract.....	xii
Chapter 1: Introduction.....	1
1.1 Inflammation, Shock, and Multiple Organ Failure.....	1
1.2 Role of the Intestine and the Gut-Lymph Hypothesis.....	2
1.3 Enzymatic Activity and Its Role in Shock.....	5
1.4 Cell Death in Shock.....	6
1.5 Role of the Vermiform Appendix and Cecum.....	7
1.6 Research Goals.....	10
1.6.1 Objective and Experimental Design.....	10
1.6.2 Hypothesis.....	11
1.6.3 Specific Aim.....	12
Chapter 2: Experimental Study.....	13
2.1 Materials and Methods.....	13
2.1.1 Animals and Tissue Collection.....	13
2.1.2 Tissue Homogenization and Colorimetric Plate Assay.....	14
2.1.3 Reverse Gelatin Zymography.....	15
2.1.4 High-Performance Liquid Chromatography and Mass Spectroscopy....	19
2.1.5 Western Blot.....	22
2.1.6 Data Analysis.....	25
2.2 Results.....	28
2.2.1 Colorimetric Plate Assay.....	28
2.2.2 Reverse Zymography Results.....	29

2.2.3 High-Performance Liquid Chromatography and Mass Spectroscopy Results.....	30
2.3 Discussion.....	50
2.3.1 Colorimetric Plate Assay.....	50
2.3.2 Reverse Zymography Results.....	52
2.4 Conclusion.....	55
References.....	56

## LIST OF FIGURES

- Figure 2.1:** A photograph of detached rat intestines, starting with the distal end of the small intestine, or ileum, down to the end of the rectum. Cuts were made at 15 cm from the junction between the ileum and cecum for small intestine, the entirety of the cecum, and about 6 cm from the end of the cecum to the colon for the large intestine....26
- Figure 2.2:** A plot of trypsin activity using the substrate BAPNA. The absorbance, which corresponds to activity level, is plotted as a function of time in minutes. Note that for the highest curve, the small intestine, the curve shows an initial linear slope until around 75 min, when it starts to flatten out.....27
- Figure 2.3:** Average activity levels of the three harvested intestinal homogenates based on absorbance; small, intestine, cecum, and large intestine. Each organ is further subdivided into three groups representing luminal material, the entire organ (wall plus luminal content), and intestinal wall only.....31
- Figure 2.4:** Average chymotrypsin activity based on absorbance measurements. There is very high variation in the small intestine measurements for luminal material and full organ, albeit with small sample size. There were no significant differences amongst the groups.....32
- Figure 2.5:** Average elastase activity based on absorbance measurements. There is very high variation in the small intestine measurements for luminal material and full organ. No significant differences were found amongst the groups, although p-values between the full organ versus cecum and full organ versus large intestine.....33
- Figure 2.6:** Average activity levels of trypsin for animals greater than 500 g body weight. The same trends hold as with the younger animals; significant differences ( $p < 0.05$ ) were evident between the small intestine versus cecum, and small intestine versus large intestine. Luminal content data was not included in this graph.....34
- Figure 2.7:** Average activity levels of chymotrypsin for animals greater than 500 g. The same trends hold as with the younger animals; no significant differences were found between groups. Luminal content data was not included in this graph.....35
- Figure 2.8:** Average activity levels of elastase for animals greater than 500 g. The same trends hold as with the younger animals; significant differences ( $p < 0.05$ ) were found between small intestine complete organ versus cecum and large intestine. Luminal content data was not included in this graph.....36
- Figure 2.9:** Average trypsin activity levels for animals between 200 to 400 g in weight. The difference between these groups versus those in Figure 2.4 is the fact that the large intestine and wall samples were harvested about 2-4 cm from the end of the cecum as opposed to the junction.....37



<b>Figure 2.10:</b> Average trypsin activity levels for animals between 200 to 400 g in weight. As with Figure 2.09, the large intestine and wall samples were harvested about 2-4 cm from the end of the cecum as opposed to the junction.....	38
<b>Figure 2.11:</b> A curve of absorbance at 595 nm versus protein concentration in $\mu\text{g/mL}$ using a BCA assay. The data are linear, and the resulting equation of the curve was used to determine protein concentrations of nine intestinal wall homogenates.....	39
<b>Figure 2.12:</b> A 15% substrate-less gel with samples of intestinal wall homogenate (diluted 1:1) stained in 0.025% Coomassie Blue. <b>A:</b> protein ladder; <b>B:</b> small intestinal homogenate; <b>C:</b> cecal wall homogenate; <b>D:</b> large intestinal wall homogenate; and <b>E:</b> undiluted aprotinin (1.4 mg/mL).....	41
<b>Figure 2.13:</b> A 12% substrate-less gel with samples of intestinal wall homogenate (diluted 1:1) stained in 0.025% Coomassie Blue. <b>A:</b> protein ladder; <b>B:</b> small intestinal homogenate; <b>C:</b> cecal wall homogenate; and <b>D:</b> large intestinal wall homogenate.....	42
<b>Figure 2.14:</b> Image of a reverse zymogram with homogenates diluted 1:1. <b>A:</b> cecum (full organ) homogenate; <b>B:</b> cecal wall homogenate; and <b>C:</b> cecal luminal content homogenate. There is a noticeable Coomassie-stained band at the center of the gel corresponding to a $\sim 25$ kDa band, in Figure 2.11.....	43
<b>Figure 2.15:</b> Image of a reverse zymogram using five different dilutions of cecal wall homogenate (derived from the same homogenate). In ratio of dilution: <b>A:</b> 1:1, <b>B:</b> 1:2, <b>C:</b> 1:3, <b>D:</b> 1:4 (oldest prepared sample; the other samples were prepared weeks afterward on the same day), and <b>E:</b> 1:5.....	44
<b>Figure 2.16:</b> A reverse zymogram of wall homogenates of equal protein concentration by order of magnitude diluted 1:1. The lanes and amount of protein placed into the lanes are: <b>A:</b> small intestine wall – 10 $\mu\text{g}$ ; <b>B:</b> small intestine wall – 20 $\mu\text{g}$ ; <b>C:</b> cecal wall – 10 $\mu\text{g}$ ; <b>D:</b> cecal wall – 20 $\mu\text{g}$ ; <b>E:</b> large intestine wall – 10 $\mu\text{g}$ .....	45
<b>Figure 2.17:</b> A reverse zymogram of wall homogenates of equal protein concentration by order of magnitude diluted 1:1. The lanes and amount of protein placed into the lanes are: <b>A:</b> small intestine wall – 10 $\mu\text{g}$ ; <b>B:</b> small intestine wall – 20 $\mu\text{g}$ ; <b>C:</b> cecal wall – 10 $\mu\text{g}$ ; <b>D:</b> cecal wall – 20 $\mu\text{g}$ ; <b>E:</b> large intestine wall – 10 $\mu\text{g}$ (in well).....	46
<b>Figure 2.18:</b> A reverse zymogram of two cecal wall homogenates incubated overnight in 10x the amount of trypsin normally used in the developing buffer. Both <b>A</b> and <b>B</b> have the same protein concentration.....	47
<b>Figure 2.19:</b> A histogram of the average trypsin activity in samples of intestinal wall homogenates mixed with an equal volume of trypsin, as well as trypsin and wall homogenate controls. Pilot studies showed that 50 $\mu\text{g/mL}$ of trypsin offered the best absorbance curve .....	48

## LIST OF TABLES

**Table 2.1:** Protein concentrations determined by BCA assay for nine sets of intestinal homogenate samples corresponding to three animals. Abbreviations are as follows; SI: small intestine, Lum: luminal content, Cec = cecum, and LI = large intestine.....40

**Table 2.2:** A chart showing the names of various proteins found in a sample of HPLC-purified cecal wall homogenate. The name of the protein is listed on the left column, while the name of the species is listed on the right column.....49

## ACKNOWLEDGMENTS

First and foremost, I would like to acknowledge my advisor and Principal Investigator, Professor Geert Schmid-Schönbein. He is the man most responsible for my growth as a scientist and investigator, and his integrity, friendliness, and respect for me as a student I will always remember. I really appreciate his willingness to accept me into his laboratory and the faith he put in me throughout the lengthy trials I spent working on my project. My sincerest thanks go to him for the time he put into advising me, as well as giving me feedback on writing and presentation.

I would also like to acknowledge Dr. Alex Penn for teaching me numerous laboratory techniques that I would need to conduct experiments necessary for my project. His guidance and advice through an often difficult process were invaluable in resolving problems and coming up with ideas for other possible studies. I would also like to thank him for his feedback on my laboratory presentations.

Additionally, I would like to thank Dr. Angelina Altshuler, Dr. Rafi Mazor, and Frank Delano for their assistance with various laboratory issues and for providing the occasional feedback in laboratory meetings. I would like to thank Dr. Kistler for his assistance in performing HPLC studies for my project, and Dr. Majid Ghassemian for his willingness to perform mass spectroscopy with the samples I gave him. I also want to thank Marco Santamaria for his continued support and assistance in the laboratory.

Finally, I would like to thank my family and friends for being there for me through the hard times. Their support and encouragement was instrumental in helping me complete this thesis.

ABSTRACT OF THE THESIS

**Mechanisms of Regulation for Serine Protease Activity in the Rat  
Ileocecal Junction**

by

Derek Wai Tam

Master of Science in Bioengineering

University of California, San Diego, 2014

Professor Geert W.Schmid-Schönbein, Chair

Digestive enzymes in the gut have recently been implicated as primary factors in the process of inflammatory shock. Pancreatic serine proteases have been determined as key players in causing damage to an ischemic intestine. Most studies have focused on the pancreas and small intestine when investigating enzymatic activity in the digestive tract.

They are fully activated in the small intestine, but their activity in the large intestine is reduced by a mechanism that is largely unknown.

This study is designed to investigate proteolytic activity at the transition from the small to the large intestine. Segments of rat small intestine, cecum, and large intestine were harvested. Using zymographic techniques, the protease activity of intestinal homogenates was measured with specific substrates of trypsin, chymotrypsin, and elastase. We tested whether cecal wall contains serine protease inhibitors that result in reduction of proteolytic activity in the large intestine using reverse zymography.

Results indicate that there is a significant reduction in protease activity, specifically trypsin, in the cecum and large intestine when compared to the small intestine. Reverse zymography results suggest that a previously unknown inhibitor of about 30 kDa for trypsin may be present in the cecal wall but absent in the small or large intestinal homogenates. When eluted and unpurified cecal wall homogenate sample was mixed in equal volume with trypsin, there was a noticeable reduction in trypsin activity. Mass spectroscopy results suggest an immunoglobulin heavy chain antibody may be the source of the unknown inhibitor, but further studies are needed.

# **Chapter 1: Introduction**

## **Ch 1.1 Inflammation, Shock, and Multiple Organ Failure**

Inflammation is a physiologic repair response to tissue injury or infection, such that normally inflammation will lead to resolution of the injury or infection and tissue healing.<sup>1</sup> The innate immune system, which serves as a first line of defense and causes subsequent activation of inflammatory cells, cytokines, proteases, and other components, acts as an initial line of defense.

However, it is also possible that the inflammation results in an overwhelming immune response, causing life-threatening symptoms such as widespread cell apoptosis and organ failure, often referred to as sepsis.<sup>1</sup> This inflammatory response has also been designated as systemic inflammatory response syndrome (SIRS). SIRS typically occurs in response to trauma, burns or other inflammatory processes and is characterized by symptoms such as fever, tachycardia, tachypnea, and leukocytosis.<sup>1</sup> Morbidity and mortality from severe sepsis and SIRS are caused by uncontrolled inflammatory response. In the United States alone, there are an estimated 750,000 cases of severe sepsis annually, with an average mortality rate of 26.8%.<sup>2</sup>

Shock and multi-organ failure are accompanied by severe inflammation. Evidence for markers of inflammation is detectable throughout the microcirculation, for example in the form of increased endothelial permeability, leukocyte and platelet attachment to the endothelium, production of free radicals, apoptosis, and eventually with cessation of blood flow and frank organ failure.<sup>3</sup> Shock can result from a number of factors:

trauma, hypovolemia, sepsis, tumors, temporary reduction or obstructions to blood flow, among other causes.<sup>4</sup> Even when a patient survives the initial insult or trauma, if organ failure should follow the situation can prove fatal. A large number of biochemical inflammatory mediators have been proposed, but the specific mediators causing multiorgan failure have eluded a direct identification.<sup>4</sup> One fact that is known, however, is that the inflammatory response is not restricted to the initial site of injury, but can spread to other remote organs that would otherwise exhibit few or no signs of dysfunction.<sup>5,6</sup>

Shock is often accompanied by inadequate tissue perfusion and oxygenation, or ischemia.<sup>7</sup> Systemic inflammation and multiple organ failure are often the end results of shock if left untreated. This organ failure may be a result of endogenous inflammatory mediators produced in the inflammatory response as opposed to exogenous factors.<sup>8</sup> Indeed, following trauma, the cause of death is likely to result from multiorgan failure. Currently, too little is known regarding the trigger mechanisms that lead from initial trauma to eventual multiorgan failure to allow for effective diagnosis and treatment.<sup>8</sup>

## **Ch 1.2 Role of the Intestine and the Gut-Lymph Hypothesis**

For many decades the gastrointestinal tract has been implicated as a primary contributor to shock.<sup>9,10</sup> Recently we hypothesized that digestive enzymes produced in the pancreas play a key role in the initiation of the inflammatory response, in a process referred to as autodigestion.<sup>4,6,9</sup> Pancreatic proteolytic enzymes digest most food during transport through the lumen of the small intestine, and are degraded by pancreatic enzymes into bioactive fragments in the intestinal lumen.<sup>9,11</sup>



Most of the pancreatic proteases are serine proteases, and possess the serine residue SER-195 involved in hydrolytic bond cleavage. Produced in the exocrine cells of the pancreas, serine proteases are stored in inactive membrane-bound vesicles known as zymogens, and are activated by enterokinases upon entering the duodenum.<sup>9,12</sup> To prevent self-digestion, the body compartmentalizes the enzymes in the lumen via the intestine's mucosal barrier, consisting of the mucin layer and the tight epithelial barrier, also known as the brush border epithelium, which is normally impermeable to digestive enzymes.<sup>9,12</sup> The autodigestion hypothesis states that pancreatic enzymes leak into the interstitial space of the intestinal wall after the intestine's mucin layer and the tight epithelial barrier are compromised during shock, and proceed to digest the intestinal tissue down to the muscle tissue layer and even into the venous circulation.<sup>6,13,14</sup>

Ischemia in the gut leads to an increased permeability of the intestinal mucosa, followed by damage and inflammation in the gastrointestinal tract.<sup>10</sup> Digestive enzymes can enter the intestinal wall to initiate autodigestion following the increase in wall permeability.<sup>15</sup> Furthermore, it has been demonstrated that the ischemic intestine possesses cytotoxic mediators that are otherwise not present in normal intestine.<sup>10</sup> Inhibiting enzymatic activity in the intestinal lumen during ischemia reduces the presence of inflammatory mediators and improves shock symptoms and outcomes.<sup>11,16,17</sup>

A phenomenon related to shock is ischemia-reperfusion injury, which can also generate inflammatory mediators in local organs, such as the intestine, and compromise cardiac function.<sup>14,18</sup> Reperfusion of the ischemic intestine with restoration of blood flow after ischemia results in cell damage via escape of digestive enzymes into the wall of the

intestine and proteolytic cleavage of the extracellular matrix.<sup>6</sup> Free radicals are released which damage cell membranes, further instigating the release of additional free radicals, cytotoxic products, and proteases.<sup>19,20,21</sup> Digestive enzymes such as trypsin and chymotrypsin have been found to play key roles activating leukocytes and altering leukocyte morphology.<sup>10,14</sup> Degradative enzymes, including proteases, also initiate pancreatitis, and may be involved in inflammatory bowel disease, diabetes, pancreatic cancer, among other disorders.<sup>12,22,23,24</sup>

During ischemia-reperfusion injury in the intestine, the luminal content of the intestine can enter the intestinal wall, generating a systemic inflammation and systemic organ damage. Three major candidates involved in the inflammation generated by luminal material from the intestine are bacteria, digested food, and digestive enzymes.<sup>10</sup>

For many decades, bacteria were hypothesized to be the primary initiators of shock. It was proposed that intestinal bacteria and their byproducts, such as endotoxin, translocate by passing across the intestinal barrier and into the circulation, resulting in inflammation and sepsis.<sup>4,22,25</sup> However, many studies have been unable to pinpoint a definitive role for bacterial translocation in multiorgan failure.<sup>20</sup> Furthermore, cell activation and necrosis can still occur even in the absence of endotoxin, and no correlation between endotoxin concentration and the development of the inflammatory response has been found; such research suggests that bacterial translocation and sepsis may not be the major cause of multiple organ failure.<sup>20</sup>

Digested food in the intestine has also been studied for its potential role as a source of cytotoxic mediators.<sup>10</sup> Preliminary results show that only after digestion with

luminal fluid containing pancreatic enzymes does homogenized food become cytotoxic, suggesting that inflammatory mediators may originate from digestive enzymes—as opposed to digested food.<sup>10</sup>

### **Ch 1.3 Enzymatic Activity and its Role in Shock**

The discovery that the pancreas is a source of inflammatory mediators has led to a number of studies about the phenomenon. While neither homogenates of pure pancreatic proteases and nonischemic intestine are cytotoxic, once mixed together to allow the intestinal homogenates to be digested by the proteases, cytotoxicity results and induces blebs in neutrophils.<sup>10,13</sup> Homogenates of ischemic pancreas also cause damage to the mucosal barrier in addition to inflammation and necrosis of neutrophils.<sup>14</sup> It was found that serine proteases and lipases are the major classes of proteases that result in cytotoxicity upon digestion of homogenates.<sup>20</sup>

Furthermore, the use of protease inhibitors to attenuate the inflammatory response following ischemia-reperfusion injury lends credence to the idea that enzymatic activity from proteases plays a key role in shock.<sup>6,16,17,26</sup> Inhibitors have been shown to reduce neutrophil activation and even reduce gut and lung injury.<sup>26</sup> Use of serine protease and lipase inhibitors also reduces intestinal injury and overall cell activation in the microcirculation.<sup>27</sup> Activation of circulating leukocytes during ischemia and reperfusion is also reduced, as well as initial symptoms and inflammation pertinent to multiple organ failure.<sup>15</sup>

To determine whether other organs are responsible for releasing inflammatory response activators besides the pancreas and intestine, studies were conducted to investigate this phenomenon.<sup>14,20</sup> As it turns out, the homogenates of these organs do not stimulate neutrophil activation alone but do when incubated with pancreatic proteases or lipases, often resulting in a cytotoxic response.<sup>20</sup> This evidence increasingly supports the hypothesis that enzymatic activity plays a central role in shock.

## **Ch 1.4 Cell Death in Shock**

Ischemia puts cells at risk for damage and even cell death when combined with reperfusion.<sup>28,29</sup> The particular cell death that often results is known as oncosis, a type of programmed cell death similar but different from necrosis that is characterized by swelling and membrane dysfunction in addition to cell detachment.<sup>30</sup> In the liver, for example, cell death is spurred by the activation of Kupffer cells (liver macrophages), that when activated following reperfusion, generates reactive oxygen species and proinflammatory cytokines that play a key role in the systemic inflammatory response and multiorgan failure.<sup>29,31,32</sup> The loss of ATP production in the mitochondria results in swelling, rounding, and the formation of plasma membrane protrusions known as blebs; symptoms consistent with oncosis.<sup>28</sup> Further, bleb formation after longer periods of ischemia/reperfusion inexorably results in necrotic cell death via osmotic swelling and bleb rupture.<sup>33,34,35</sup> Membrane rupture can result in the release of inflammatory mediators that contribute to the to the inflammatory response.<sup>30</sup> Ultimately, it is safe to presume that cell death is a major factor in cytotoxicity and damage caused during systemic inflammation.

## Ch 1.5 Role of the Vermiform Appendix and the Cecum

The vermiform appendix is a narrow tube attached to the posterior medial wall of the beginning of the cecum of the large intestine, forming a blind end.<sup>36</sup> The word “vermiform” is derived from Latin, meaning “worm-like,” an appropriate term since the structure itself elongates less rapidly compared to the rest of the colon during gestation, resulting in a worm-like structure.<sup>36</sup> The appendix ranges in length, from 2 to 20 cm, or 10 cm on average. Lined by colonic epithelium, the appendix wall consists of two muscle layers, inner circular and outer longitudinal.<sup>37,38</sup> Presently little is known regarding the actual function of the appendix, which was once thought to be a vestigial organ, but it has been proposed that the appendix serves a primarily immunological purpose.<sup>37</sup> For instance, it is now proposed that the appendix guards the small intestine from bacteria present in the large intestine.<sup>39</sup> Other potential functions include embryological, physiological, bacteriological, and biochemical mechanisms.<sup>36</sup>

There is some evidence as to the embryological and physiological functions of the appendix. The appendix grows rapidly during the fifth and sixth weeks of fetal development, growing finger-like villi on the interior surface.<sup>40</sup> In addition, the goblet cells in the appendix secrete a type of mucosal layer containing a high concentration of IgA type immunoglobulins that may play a role in both surface immunity and the bowel-blood barrier.<sup>41,42</sup> Furthermore, primarily acid mucin layers exist in the cecum, appendix, and large intestine.<sup>43</sup>

The appendix's bacteriological role is controlling the essential bacteria residing in the cecum and colon, particularly during the early stages of life.<sup>38</sup> There are hints that the appendix may develop systemic tolerance to antigenic agents derived from bacteria, food waste, or even proteolytic enzymes.<sup>41,42,44</sup> Regarding a biochemical role, it has also been found that about one in 300 appendectomy specimens contains a carcinoid tumor with vaso-active cell types such as serotonin, which happens to occur in the appendix only.<sup>37</sup> This would suggest some correlation between the appendix and these cell types.

Current research suggests that the appendix's primary functions are immunological, as the appendix contains numerous specialized lymphoid follicles, which are involved in antibody production.<sup>38,39,41,42,44</sup> The antibodies are as follows: IgA immunoglobulins, which provide secretory and mucosal surface immunity, IgM and IgG immunoglobulins, which grant bloodstream and humoral immunity.<sup>38,39,41,42,44,45,46</sup>

In contrast to these functions, the purpose of this current study is to elucidate the possible role of the appendix in regard to proteolytic activity in the large intestine.

A small number of bacteriological studies have investigated the cecum and large intestine of animals such as rats, For instance, one rat study on cirrhosis, a liver disease sometimes caused by enteric bacteria, found that bacterial translocation in the cecum was the likely factor responsible for the development of spontaneous infections in cirrhosis.<sup>47</sup> There is also mounting evidence of enzymatic activity and its role in carcinogenesis in the gastrointestinal tract. Serine proteases such as trypsin have also been implicated in the progression and metastasis of tumors in the digestive tract.<sup>48,49,50,51</sup> In addition, it was reported that serine protease inhibitors suppress carcinogenesis both *in vivo* and *in*

*vitro*.<sup>52,53</sup> Another study revealed that the protease-activated receptor-2 (PAR-2), which acts as a mediator of trypsin, plays a role in the proliferation of colon cancer cells in culture.<sup>54</sup> Thus, it would seem that proteolytic activity does play a largely debilitating role not just in the small intestine and pancreas, but also in the large intestine.

Concerning the role of the appendix in secreting antibodies, a number of studies have suggested that antibodies may play a role as protease inhibitors. Many proteases are targetable by antibodies since approximately half of them are extracellular.<sup>55</sup> Natural protease inhibitors possess protruding active-site loops that interact with substrate-binding clefts in a canonical manner.<sup>56</sup> In one study, Kunitz domain inhibitors were successfully engineered with camelid heavy chain antibodies, lacking a light chain, but possessing a CDR-H3 loop that allows for optimal cleft insertion into protease domains.<sup>57, 58</sup>

Studies on the antibody-binding epitope (where the antibody makes contact) of proteases revealed that the most common mode of inhibition is competitive inhibition<sup>59</sup>, though there also exists mixed-type inhibition<sup>60</sup> for certain antibodies. The first major mechanism by which antibodies inhibit proteases is via steric hindrance of substrate access to the catalytic cleft. One such antibody displaying this mechanism is the anti-HGFA antibody (Fab58), which obstructs substrate access to the active site, acting as a competitive inhibitor.<sup>61, 62</sup> The second major mechanism is allosteric inhibition, or the “allosteric switch” mechanism, by which partial inhibition is achieved via enzyme kinetics.<sup>61, 63</sup> This was evident in the Fab75-HGFA complex<sup>61</sup> and the Fab40 HGFA antibody<sup>63</sup> which does not bind to the active site region, but instead a conformational

change in an HGFA loop enables the ‘switching’ on or off to enable an ‘enzymatically active’ competent state or ‘catalytically inactive’ non-competent state.<sup>56</sup> Depending on the equilibrium of the competent state, catalysis can either proceed as normal or be inhibited in the non-competent case.<sup>56</sup> Further, the allosteric sites have high specificity for antibodies directed against them, while inhibitors are protected from inadvertent proteolysis due to the epitope being located outside the catalytic cleft.<sup>56</sup>

## **Ch 1.6 Research Goals**

### **Objective and Experimental Design**

Based on current knowledge about the inflammatory cascade and multiple organ failure in shock, we seek to further investigate the effects of enzymatic activity in the digestive system. Digestive enzymatic activity may be one of the primary causes of cell death and organ damage following ischemia-reperfusion injury. Most current studies have focused on the pancreas or the small intestine when investigating the digestive enzymatic activity in the digestive track, and it is unclear to what degree the digestive enzymatic activity continues as food items are transported from the small into the large intestine. In particular, it is important to know the level of proteolytic activity, upon passage through the ileocecal junction between the small intestine and the cecum of the large intestine. Research into this issue may provide another window into the physiological role of the vermiform appendix.

This study was designed to investigate the proteolytic activity at the transition between the small intestine and the large intestine. An initial pilot study suggested that



the activity levels of various serine proteases in the small intestine, cecum, and large intestine of Wistar laboratory rats exhibit a significant reduction in serine protease activity levels in the cecum and large intestine compared with the levels in the small intestine (see Results). Thus, we hypothesize that proteolytic activity decreases significantly in the cecum and large intestine by a mechanism that involves the cecum.

Activity levels of various pancreatic serine proteases in samples of rat intestinal homogenates were measured by zymographic techniques. A reverse zymography technique was then used to determine whether a serine protease inhibitor(s) was causing the attenuation in activity in the lumen of the cecum and large intestine. After further purification, the inhibitor of interest can be isolated by high-performance liquid chromatography and identified by mass spectroscopy. Western blot studies suggest the possibility of an enzymatic degradation of digestive enzymes in the cecum and large intestine. The overall goal of the research is to bring to light a possible new molecule or mechanism that may protect the large intestine against damage caused by digestive enzymes.

## **Hypothesis**

In this study, we hypothesize that the proteolytic activity of the serine proteases in the cecum and large intestine decreases as compared to the small intestine due to the presence of enzymatic inhibitors or enzyme degradation. The decrease in protease activity is brought about by secretion of a protease inhibitor from the wall of the cecum (the counterpart to the appendix in humans). The resulting attenuation in the activity levels of these proteases is the large intestine's potential defense mechanism against

digestive enzymes; since food items are dehydrated in the large intestine, active enzymes would be further concentrated and may cause damage to the structure of the large intestine unless digestive enzymes are blocked.

### **Specific Aim**

Analyze protease activity levels of intestinal homogenates of rat small intestine, cecum, and large intestine using zymographic techniques. Utilize reverse gelatin zymography to determine whether or not a serine protease inhibitor is present in the sample of cecum or large intestine homogenate. Utilize Western blot techniques to determine whether enzymatic degradation plays a role by measuring for the presence of a protein gradient. If present, determine the molecular weight of the inhibitor, and its sequence to potentially match this inhibitor with known serine protease inhibitor profiles.

## **Chapter 2: Experimental Study**

### **Ch 2.1 Materials and Methods**

#### **Ch 2.1.1 Animals and Tissue Collection**

Male Wistar rats, fed a diet of standard laboratory chow (8604 Teklad Rodent Diet, Harlan Laboratories, Indianapolis, IN) and water, weighing between 200 to 400 grams were anesthetized with a combination of Ketamine and Xylazine (10 mg/mL, 115  $\mu$ L/kg body weight i.m.) (MWI, Nampa, ID) in a ratio of 7.5  $\mu$ L: 4  $\mu$ L. After at least 10 to 12 minutes, reflex level of the rat was tested via toe pinch. Responsive animals were given an additional waiting period of 5 to 10 minutes before retesting. Using this test, all animals utilized in the study were determined to be fully anesthetized following the waiting period.

Terminal surgery was performed following anesthesia. First, the rats were securely placed over a cutting board resting atop a heating pad at 37°C. After shaving off the abdomen and most of the proximal torso, a midline incision was made, with care taken not to damage internal organs. Then the small intestine, cecum, and large intestine were gently exteriorized and placed over a saline-dampened gauze pad lying adjacent to the rat. The animal was then euthanized with an injection of 400  $\mu$ L of B-Euthanasia and selected sections of the intestines were harvested. Following this procedure, a roughly 15 cm distal end of the small intestine (the ileum) was collected and divided into two halves. This was repeated for the entire cecum and the proximal end of the large intestine (roughly 6 cm in length); see Figure 1 for photographs of each section.

After rinsing both sections in saline solution, one section was placed into a pre-weighed 50 mL tube and immediately stored in a liquid nitrogen container for quick freezing. The tubes were weighed prior to surgery to ensure accurate w/v measurements for homogenization. The other section was carefully cut longitudinally so that luminal contents were exposed. It was then placed in a 50 mL tube with 40 mL of saline and inverted vigorously to release the luminal content. Once the tissue was removed from the tube, the procedure was repeated at least once with another 50 mL tube of saline before the flushed intestine was placed in an empty 50 mL tube, which was then immediately frozen in liquid nitrogen. Some leftover luminal content were also added into a 15 mL tube and frozen. The rinsing and storing in liquid nitrogen was repeated for the whole cecum and the proximal end of the large intestine, including their luminal content. After all samples were collected, the tubes were removed from the liquid nitrogen container and stored at  $-80^{\circ}\text{C}$  to preserve protease activity until they were homogenized.

### **Ch 2.1.2 Tissue Homogenization and Colorimetric Plate Assay**

Usually within two days of surgery and storage at  $-80^{\circ}\text{C}$ , the intestine samples were homogenized using a Polytron P1200 tissue homogenizer. First, phosphate buffered saline (PBS) was added to the sample tubes based on the dry weight of the tissue, in a ratio of roughly 1:4 w/v (in g/mL). Then the thawed tissues were homogenized while the tubes sat on ice. 2 mL aliquots of the homogenates were taken and stored at  $-80^{\circ}\text{C}$  until use for analysis by plate reader or gel electrophoresis.

The intestinal homogenates were analyzed using a microplate reader, the FilterMax F5. Samples were analyzed for the presence of three serine proteases: trypsin,

chymotrypsin, and elastase. Protease activity was determined by measuring the absorbance of the following fluorescent substrates: BAPNA (N-alpha-benzoyl-DL-arginine-p-nitroanilide), SAPNA (N-Succinyl-Ala-Ala-Pro-Phe p-nitroanilide), and SAAPLPNA (succinyl-ala-ala-pro-leu-p-nitroanilide) for trypsin, chymotrypsin, and elastase, respectively. Prior to the plate analysis, 20  $\mu$ L of undiluted intestine homogenate was added to 180  $\mu$ L of substrate on a 96-well microplate. Leftover homogenates were returned to storage at  $-80^{\circ}\text{C}$ . Samples were measured in triplicate, corresponding to the full organ (wall plus luminal content), rinsed intestinal wall (without luminal content), and luminal content for the small intestine, cecum, and large intestine (a total of nine samples). PBS was used as a negative control.

The samples on the plate were analyzed using a 405-nm wavelength protocol with 15-min measurement increments for a total of three hours. Thirteen time points were selected to generate a time course of absorbance. Activity levels were determined by the amount of absorbance, and then single-factor ANOVAs and paired t-tests were performed to compare differences between the individual intestinal organs and luminal content.

### **Ch 2.1.3 Reverse Gelatin Zymography**

#### *Preparation of Gels*

Based on the initial results of the pilot study and the colorimetric plate analysis, we hypothesized that a potential serine protease inhibitor is present in the rat cecum homogenate. To this end, an SDS-PAGE reverse zymography using gelatin as the substrate was performed. Polyacrylamide gels ranging in composition from 10% to 15%

were tested. It was found that 15% gels were best suited for viewing the control protease inhibitor, aprotinin. Aprotinin, a trypsin inhibitor, has a molecular weight ranging from 5 to 15 kDa, which appears near the bottom of a 15% gel. Briefly, the protocol is as follows.

First, a separating gel, or lower gel, was created using a combination of DI water, 30% Bis-Acrylamide, 0.375M Tris-HCl at pH 8.8, 0.1% SDS, 0.1% gelatin (1 mg/mL), 10% ammonium persulfate (APS), and tetramethylethylenediamine (TEMED). The latter two ingredients were added following a 15 min incubation of the solution in a 37°C hot water bath. Afterwards, the gel monomer solution was placed between two glass plates (a spacer plate and a short plate, forming a gel cassette) mounted on a Bio-Rad Mini-PROTEAN Tetra Cell casting frame, which is then mounted on a casting stand. The stand allows for the mounting of two Minigels; thus, two gels were run per experiment. DI water was added over the gel to prevent potential dehydration. After a waiting period of about 10 min, the gel was confirmed to have polymerized and solidified between the plates.

Next the stacking gel, or upper gel, was generated by mixing DI water, 30% Bis-Acrylamide, 0.330M Tris-HCl at pH 6.8, 0.1% SDS, 10% APS, and TEMED. It was added over the polymerized separating gel and to the top of the short plate, and immediately a 9 or 10-well comb was placed over the stacking gel, with care taken to avoid bubbles. After some time, the upper gel was determined to have polymerized and the combs were carefully removed.

### *Sample Preparation and Electrophoresis*

Meanwhile, cecum homogenate samples from -80°C storage were prepared and diluted to ensure clear visualization in the gel. During some pilot studies, it was determined that a roughly 1:1 dilution with PBS allowed for best visualization of the sample in the gel. Multiple samples from different animals were placed alongside a positive control, aprotinin, which was kept undiluted at 1.4 mg/mL. Samples were mixed with 4x loading buffer (pre-made and provided by Bio-Rad) prior to addition to the wells. The loading buffer served as a dye marker while the samples ran down each lane.

Next, the gel cassette sandwich were removed from the casting stand and placed on an electrode assembly, which consists of a sealing gasket and anode and cathode. The assembly was then placed in a mini tank, which houses two assemblies. 1x gel running (electrode) buffer, consisting of Tris base, glycine, SDS, and DI water, was then poured over the assemblies to fully submerge the gels. Afterward the gels were run by attaching the lid over the tank and electrode assemblies, and then connected to a DC voltage power supply. Gel electrophoresis was run initially at 80 V for the first 20 min, then at 120 V for the remaining time. Gels typically ran around 75 to 90 min before the bromophenol blue dye from the loading buffer reached the bottom of the gel.

Occasionally, a substrate-less gel was run alongside a single reverse zymogram. This gel was made using the same recipe as mentioned in the previous section, only without a gelatin substrate. In addition to all the homogenate samples run in the reverse zymogram, a Benchmark<sup>®</sup> protein ladder was added to the first lane, serving as a marker to determine rough molecular weights of each visualized band. The purpose of the

substrate-less gel was to act as a comparison with the reverse zymogram in order to determine the corresponding molecular weight of any bands that appear on the reverse zymogram, since protein ladder does not appear in reverse zymograms. Furthermore, this would differentiate between bands that appear in the substrate-less gel versus the reverse zymogram; i.e. which bands could be a potential inhibitor versus those that are not.

#### *Renaturation and Gel Development*

Following electrophoresis, the gels were removed from the electrode assembly and carefully extracted from the space between the plates with a spatula. Each gel was then placed in a gel container filled about halfway with renaturing buffer, consisting of 2.5% Triton-X buffer in DI water. The renaturing buffer serves to renature protease molecular bonds that were broken during gel electrophoresis. Gels were then agitated in 15 min increments for a total of one hour on a shaker. Between each cycle, renaturing buffer was removed and replaced in the container. The substrate-less gels were *not* put in renaturing buffer, and instead were stained immediately following electrophoresis (for details see the following section).

After renaturing, the gels were rinsed once with reverse zymography developing buffer consisting of water, 10 mM Tris base, 200 mM NaCl, 10 mM dehydrated CaCl<sub>2</sub>, 0.02% Brij-35, and 5 µg/mL of trypsin. Then 40 mL of developing buffer was poured into each gel container, and the gels were allowed to incubate overnight (12-16 hrs) in a 37°C hot water bath. The trypsin in the buffer digests the gelatin during the incubation phase, causing the gel background to turn clear and ensuring that only inhibitor bands rather than normal protease bands can be visualized.



### *Staining and Destaining of Gels*

After overnight incubation, the gels were removed from the gel containers and replaced in a transparent plastic container partially filled with staining buffer. The buffer consists of water, methanol, acetic acid, and 0.025% Coomassie blue. The gels were washed once with the buffer, re-submerged in staining buffer, and then placed on an agitator for three hours. Following this step, the gels were washed with destaining buffer consisting of water, methanol, and acetic acid, and then returned to the agitator. After 10 to 20 min, if the gel was still too blue, the destaining buffer was replaced. The gel was removed from destaining solution and replaced in DI water once blue bands were clearly visible. Destaining in water could continue overnight for improved band visualization. Inhibitors to trypsin will appear as a dark band on a clear background. The gels were positioned between transparent films and scanned afterwards to allow for analysis.

### **Ch 2.1.4 High-Performance Liquid Chromatography and Mass Spectroscopy**

#### *Silver Staining and Protein Elution*

In order to prepare the cecal wall samples for mass spectroscopy, the samples had to be further purified due to high protein content. The band containing the potential inhibitor of interest was first isolated using a simple protein elution technique. First, two SDS-PAGE Mini-gels were run via electrophoresis. Afterwards, one of the gels (containing a protein maker) was silver stained to determine locations of protein bands, while the other gel was kept hydrated. Silver staining is a technique allowing for protein identification at high sensitivity.

Briefly, the silver staining protocol is described as follows: first, the gel was taken from the cassette, placed in a staining tray, and rinsed briefly in ultrapure water. Next, the gel was fixed in fixative for 20 minutes to remove interfering ions and detergents from the gel, and then washed in 30% ethanol for 10 minutes. Afterwards, the gel is incubated for 10 minutes in sensitizing solution to improve staining contrast. After washing again in 30% ethanol and ultrapure water for a total of 20 minutes, the gel is incubated in staining solution for 15 minutes, and then washed for 30 seconds in ultrapure water. The gel was then placed in Developing solution for 4-8 minutes until the appearance of bands of the desired intensity. Finally, Stopper solution is added directly to the gel in Developing solution, and agitated for 10 minutes before a final 10 minute ultrapure water wash step.

Following staining, the protein band corresponding most closely with the Coomassie Blue-stained inhibitor band of interest from reverse zymography was excised from the second, unstained gel (the location of the band was matched to that of the stained gel) using a clean razor blade. The gel strip was further cut into smaller bands so as to be able to fit into a 2-mL microcentrifuge tube. Next, the protein was purified from the gel matrix by first placing the excised gel pieces into the tube, and adding about 0.75 to 1 mL of elution buffer (50 mM Tris-HCl, 150 mM NaCl, and 0.1 mM EDTA at pH 7.5) to completely immerse the gel strips. Then the strips are crushed in solution with a 1-mL syringe and incubated on a rotary shaker at about 30°C overnight. Finally, the solution is centrifuged at 10,000 *g* for 10 minutes and the supernatant is added to a new centrifuge tube, which can then be used for high-performance liquid chromatography.

### *High-Performance Liquid Chromatography*

High-performance liquid chromatography, also known as HPLC, is a chromatographic, mass transfer technique used to separate and purify individual compounds in a mixture or solution.<sup>55</sup> This technique utilizes adsorption via high-pressure pumps that pass a pressurized liquid (the mobile phase) and sample mixture through a column of sorbent (stationary phase), wherein the components are separated. The particular method used in this experiment was reversed-phase HPLC, in which the stationary phase is non-polar and hydrophobic while the mobile phase is somewhat polar. Hydrophilic, polar molecules elute more quickly, thereby separating the mobile from the stationary phase. Retention time can be adjusted based on the hydrophobic interactions of the analyte.

Following HPLC analysis, fractionated samples of each “peak” are analyzed using plate zymography. The sample is measured both separately against a trypsin control and combined in equal parts to the same trypsin sample, in order to determine if a decrease in trypsin activity occurs when trypsin is combined with the HPLC sample.

Some samples were run without HPLC analysis and instead underwent plate zymography following elution from the SDS-PAGE gel. The same protocol was followed as with the HPLC samples.

### *Mass Spectroscopy*

Mass spectroscopy (MS) is a common technique used to determine the elemental composition of a sample based on the masses of molecules and chemical compounds.

Charged particles are generated when these compounds are ionized, with the resulting byproducts separated according to their mass-to-charge ratio. The ions are then detected with a mass spectrometer and the signal is processed into a spectrum of masses of all molecules in the sample. Subsequent data analysis allows one to determine the amino acid sequence of proteins and other molecules, in this case, the inhibitor of interest.

### **Ch 2.1.5 Western Blot**

#### *BCA Protein Assay*

In order to determine whether enzymatic degradation from the transition between the small intestine and cecum and large intestine plays a role in the reduction of activity at the ileocecal junction, a Western blot was performed to determine trypsin levels in the proteins of the intestinal homogenates. Prior to running a Western, a BCA (bicinchoninic acid) protein assay, intended to measure protein concentration of each homogenate sample, served as an initial analysis. This assay involved comparing diluted samples of intestinal, wall, and luminal content homogenates with several albumin standards in order to construct a protein concentration curve based on measured absorbance at 595 nm wavelengths. To ensure enzymatic activity, samples were incubated at 37°C in a water bath prior to placement into a microplate. After cooling to room temperature, the absorbance was then measured on a plate reader.

#### *Electrophoresis and Membrane Transfer*

Following BCA protein analysis, concentrations of each homogenate sample to be run on the Western blot were standardized such that the concentration in each sample

would be fixed and identical to one another. All samples that required dilution to reach the desired concentration were diluted with PBS. An SDS-PAGE polyacrylamide gel was run including all homogenate samples using the protocol outlined in the previous section on Electrophoresis (Paragraph 3, for substrate-less gels), with the notable exception of 2.5%  $\beta$ -mercaptoethanol used in the sample buffer to ensure reduction and denaturation of proteins and to maintain their activity. After combining the samples with buffer in 1:2 ratios, all samples were boiled at 100°C for 5 to 10 minutes. Afterwards, the samples were run on the gel as previously described, alongside a Colorburst™ Electrophoresis Marker (M.W. 800-220,000 Da) (Sigma). Resolving gels were run at 10-12%.

After electrophoresis, membrane transfer was performed. First, blotting buffer was prepared to a concentration of 1x from glycine, Tris-base, methanol, and DI water. All sponges and filter papers were prewet prior to gel removal, and PVDF membrane (Millipore Immobion-P) was used as the transfer medium. A “sandwich” assembly was then prepared using Bio-Rad’s Transblot, consisting of the gel and PVDF membrane sandwiched between filter papers and sponges. The gel(s) was carefully placed over one filter paper and kept hydrated with blotting buffer. The membrane was placed over the gel on the opposite side of the filter paper, and another filter was added over the membrane. To complete the sandwich, sponges were placed on both ends and then the assembly was sealed and placed onto a gel gasket. An ice pack was then placed next to the gasket, and 1x blotting buffer was poured onto the gel case. The gasket was then placed in a large container containing ice to maintain a temperature close to 4°C around the gel(s) to prevent overheating. The Transblot assembly was run at 100 V for one hour.

In order to prevent nonspecific binding of the primary and secondary antibodies to the membrane, membrane blocking was performed. Blocking buffer was prepared from 1x TBST (consisting of TBS, Tween20, and ultrapure water) and 5% nonfat dry milk. The TBS consisted of Tris-base, NaCl, and ultrapure water at a pH of 7.6. Following membrane transfer, the PVDF membrane, which should now contain the protein blots from the gel, was washed twice in TBST and then immersed in blocking buffer and incubated either overnight over an ice pack on a rotary shaker, or for 45 minutes on the shaker without ice.

#### *Antibodies and Detection*

Following the blocking step, the membrane was cut at approximately the locations between the 20 kDa and 45 kDa bands of the protein marker, such that the proteins of interest corresponding to the protein references trypsin (23.3 kDa) and  $\beta$ -actin (42 kDa), would be included. The rest of the membrane outside of this range of molecular weights was discarded. The membrane strip of interest was then rinsed twice in TBST and then immersed in 5 or 10 mL of blocking buffer containing primary antibody (anti-trypsin D) in a ratio of 1:1,000 antibody to buffer. The membrane was then incubated for 2.5-3 hours (or overnight) on a rotary shaker. After incubation, the membrane was washed for about 30 minutes in TBST, with four changes of buffer.

Next the membrane was incubated in TBST containing the secondary antibody (anti-mouse antibody) in a ratio of 1:10,000 (antibody to buffer), for one hour. The 30-minute membrane wash step was repeated following incubation. Using a chemiluminescent pico- or femto- detection kit, 1 mL of each ECL developing and fixing

agent (1:1 ratio) was mixed and poured over the membrane. The membrane was then placed in between two overhead slides to keep hydrated, and subsequently brought to the darkroom along with autoradiography film to develop. The pictures taken during development of the Western blot were analyzed for the presence of specific proteins.

## **Ch 2.1.6 Data Analysis**

### *Data Plotting*

Following measurement of absorbance by the fluorescent plate reader, an Excel file with all data from the 13 time points was generated. Using this data average means of each sample performed in triplicate were calculated, then normalized by subtracting initial values at time point zero, and finally corrected by subtracting the absorbance value of the PBS negative control and PBS plus DMSO substrate from the protease substrate in question. The activity profile was then plotted as a function of absorbance versus time in minutes (example curve in Figure 2.2). Finally, a bar graph was made after selecting the time point where the highest absorbance curve started to exhibit a linear trend; in most cases this was at about 75 min. Thus, the graph shows the activity level of the serine protease in question as a function of absorbance, while comparing the nine samples of intestinal homogenate and luminal content (see Results section).

### *Statistical Analysis*

For the fluorescent plate assays, two-tailed t-tests were performed between the various intestinal homogenate groups to determine statistically significant differences between groups. For example, t-tests were used to compare all wall groups; the small

intestine, cecum, and large intestine. With a relatively robust sample size of animals, comparisons were only considered significant if  $p < 0.05$ . Additionally, a single factor ANOVA was conducted to compare between groups, along with post-hoc Bonferroni, to determine whether there are significant differences in the means.

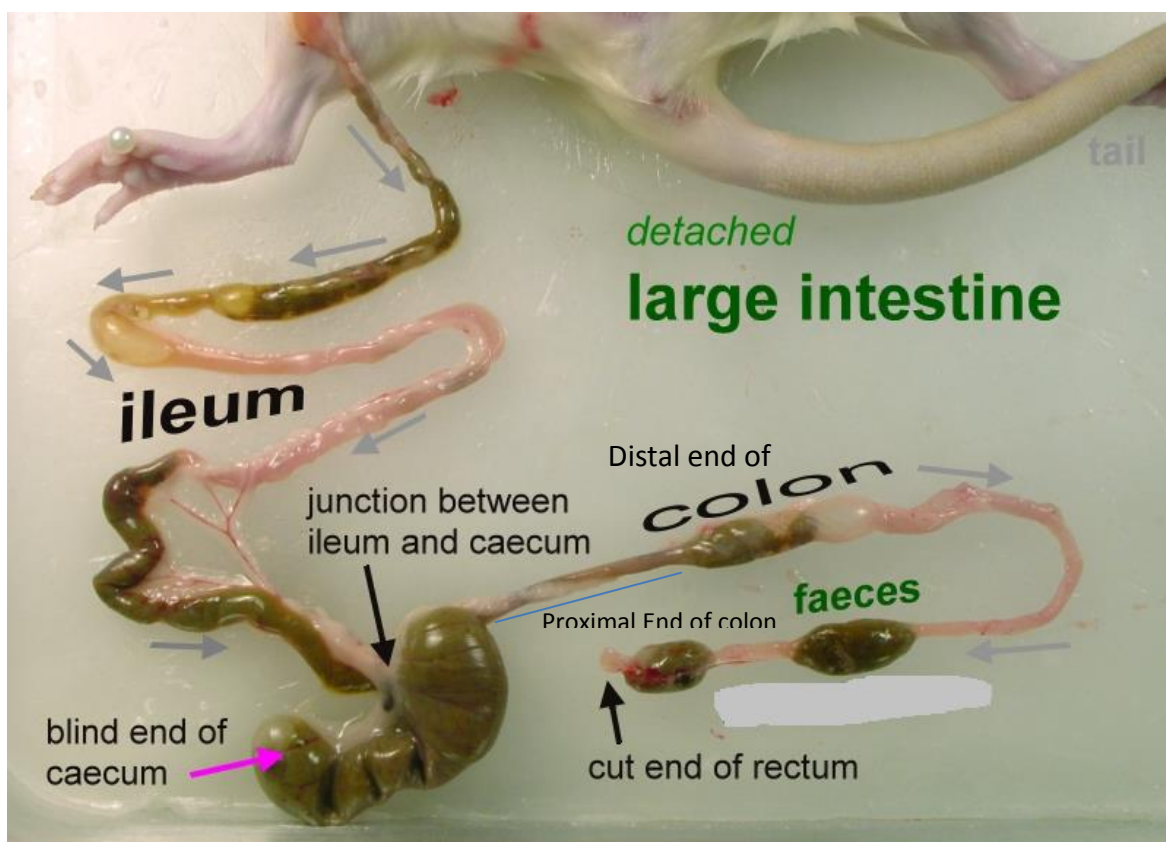


**Figure 2.1:** A photograph of detached rat intestines, starting with the distal end of the small intestine, or ileum, down to the end of the rectum. Cuts were made at 15 cm from the junction between the ileum and cecum for small intestine, the entirety of the cecum, and about 6 cm from the end of the cecum to the colon for the large intestine.<sup>1</sup>

<sup>1</sup> [http://www.ccmkc.edu.hk/~kei-kph/Rat%20dissection/Rat\\_digestive%20system.htm](http://www.ccmkc.edu.hk/~kei-kph/Rat%20dissection/Rat_digestive%20system.htm)



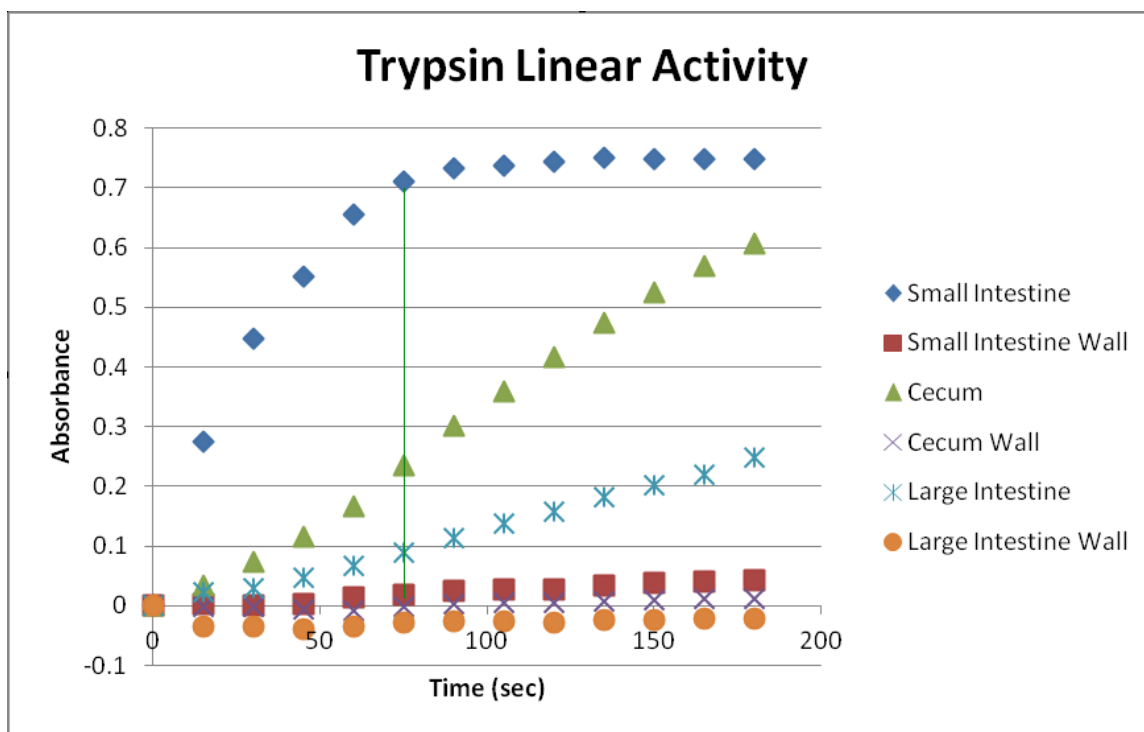


**Figure 2.2:** Time course of trypsin activity using the substrate BAPNA. The absorbance, which indicates the activity level, is plotted as a function of time in minutes. Note that for the highest curve, the small intestine, the curve shows an initial linear slope until around 75 min, when it starts to flatten out. At this time point we choose to take the value of absorbance for our data. The groups in this time course include the whole intestinal organs and wall, but not the luminal content, which are included in other plots.

## **Ch 2.2 Results**

### **Ch 2.2.1 Colorimetric Plate Assay**

For analysis of protease activity, Wistar rats weighing between 200 to 400 g were used. However, there were a number of older animals weighing at least 500 g. Due to potential differences in the two groups, data was separated according to body weights. The younger animals weighed between 200 to 400 g (around 2 to 3 months in age), and older animals (at least 3 months old) typically weighed over 500 g.

Averaged results for the three serine proteases, trypsin (Figure 2.3), chymotrypsin (Figure 2.4), and elastase (Figure 2.5), all for animals weighing between 200 to 400 g, show in all cases that there is significant reduction of protease activity in full organ homogenates from the small intestine to the cecum and the large intestine. Results for animals weighing over 500 g show a similar trend (Figures 2.6, 2.7, and 2.8).

Initial data for the large intestine was found to have high variation, which may be due to the inconsistent tissue collection along the colon. In a first sequence of studies the large intestine samples were taken closer to the end of the cecum (Figures 2.3, 2.4 and 2.5), so that the luminal content was similar in composition to that of the cecum (liquefied waste as opposed to dehydrated waste pellets).

In a later sequence of studies, samples of large intestine were harvested at least 2-4 cm away from the end of the cecum, where the luminal content was typically in solid pellet form due to dehydration. The results from the proximal and distal large intestine

were separated for trypsin (Figures 2.9), and showed also a consistent reduction of protease activity from the small intestine, the cecum, the proximal and the distal large intestine using full organ homogenates. The same trend was present for the luminal content of the small intestine versus that of the distal end of the large intestine (colon), where the luminal material was in the form of solid waste pellets. The consolidated data of all animals weighing between 200 to 400 g is shown in Figure 2.10.

For the BCA assay, a standardized curve of absorbance versus protein concentration (in  $\mu\text{g/mL}$ ) was generated (one example shown in Figure 2.11). These results only pertained to a single animal. Undiluted protein concentrations for all samples of intestinal homogenate were calculated using this curve and the data can be found in Table 1.

### **Ch 2.2.2 Reverse Zymography Results**

Substrate-less control gels were occasionally run alongside a reverse zymogram (Figures 2.12, 2.13, and 2.14). Some images were enhanced for contrast using ImageJ. Photographs of the gels following overnight incubation from reverse zymography (Figure 2.15, 2.16, 2.17, 2.18, 2.19, and 2.20) revealed a noticeable band pattern with a dilution ratio of at least 1:2 homogenate to PBS (most gels displayed were diluted 1:1, unless otherwise stated). This band is most likely a trypsin inhibitor of molecular weight around 25 to 30 kDa.

### **Ch 2.2.3 High-Performance Liquid Chromatography and Mass Spectroscopy Results**

Following elution and purification via HPLC, cecal wall homogenate samples, separated as 'peaks', were analyzed via plate zymography. However, the results showed no appreciable change in trypsin activity levels when mixed in a 1:1 ratio with 50 µg/mL of trypsin, especially when compared to an aprotinin control. Thus, we concluded that running the samples through HPLC might over-dilute the wall material such that the inhibitor activity may no longer exist. Thus, no results from HPLC are shown.

The results from the wall homogenate samples eluted directly from SDS-PAGE are shown in Figure 2.21. It was determined that when trypsin is mixed in equal volumes with eluted cecal wall homogenate, a nearly 50% reduction in activity occurred. A reduction of about 30% occurred when trypsin was combined with eluted large intestine homogenate. However, there was no meaningful reduction when combining pure, unpurified cecal wall homogenate with trypsin. When unpurified large intestinal wall homogenate was combined with trypsin, there was actually an increase in activity overall.

The results from a number of mass spectroscopy studies revealed the presence of a number of proteins, including keratin, actin, desmin, beta-globin, hemoglobin alpha 1 and 2 chains, and TAO kinase. There was also the presence of an immunoglobulin heavy chain (gamma polypeptide), as shown in Table 2.

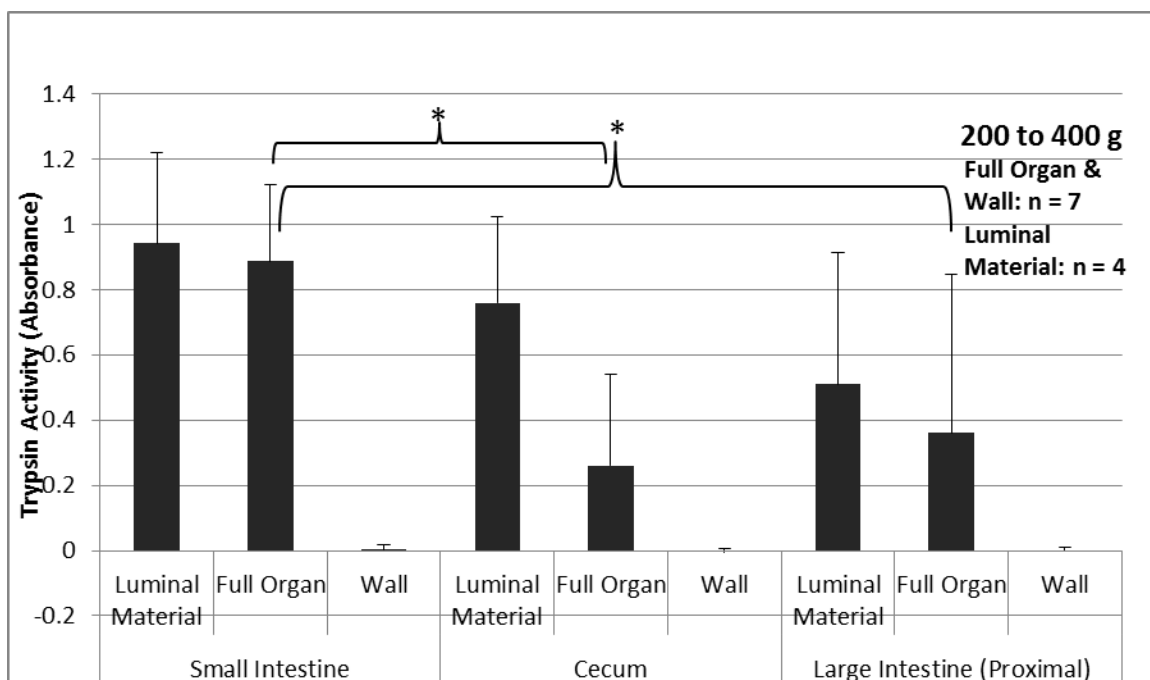


**Figure 2.3:** Average activity levels of the three harvested intestinal homogenates based on absorbance at 75 minutes; small, intestine, cecum, and large intestine. Each organ is further subdivided into three groups representing luminal material, the entire organ (wall plus luminal content), and intestinal wall only. Error bars represent mean  $\pm$  SD. \*  $p < 0.05$ , paired t-test and single factor ANOVA.

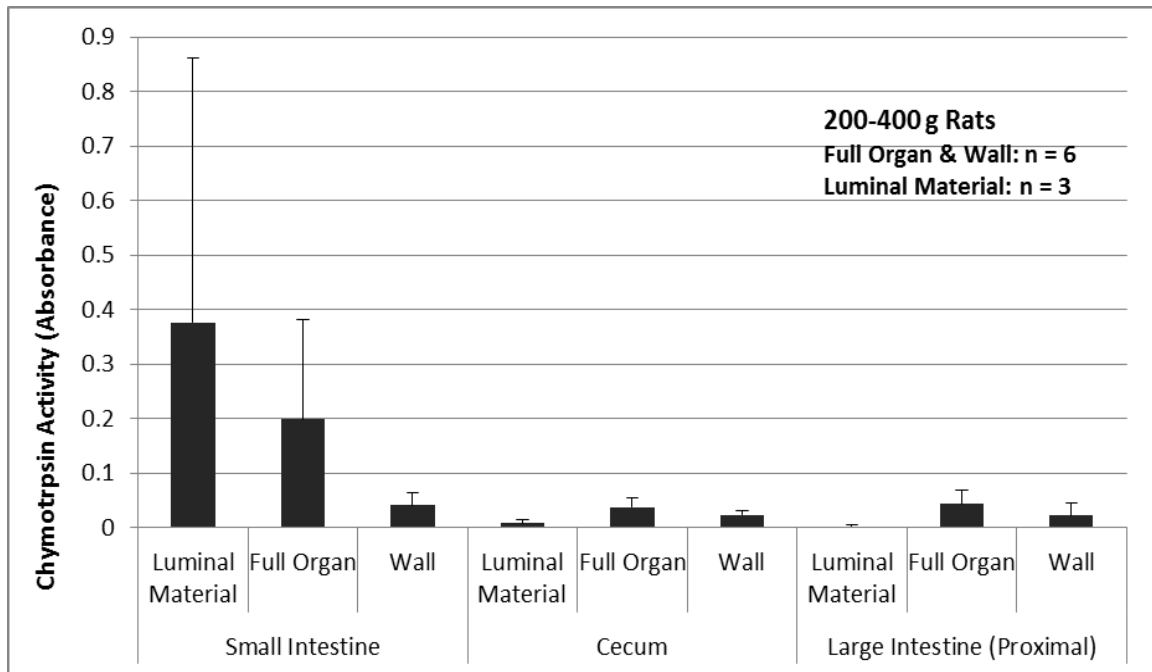


**Figure 2.4:** Average chymotrypsin activity at 180 minutes based on absorbance measurements. There is very high variation in the small intestine measurements for luminal material and full organ, albeit with small sample size. There were no significant differences amongst the groups.

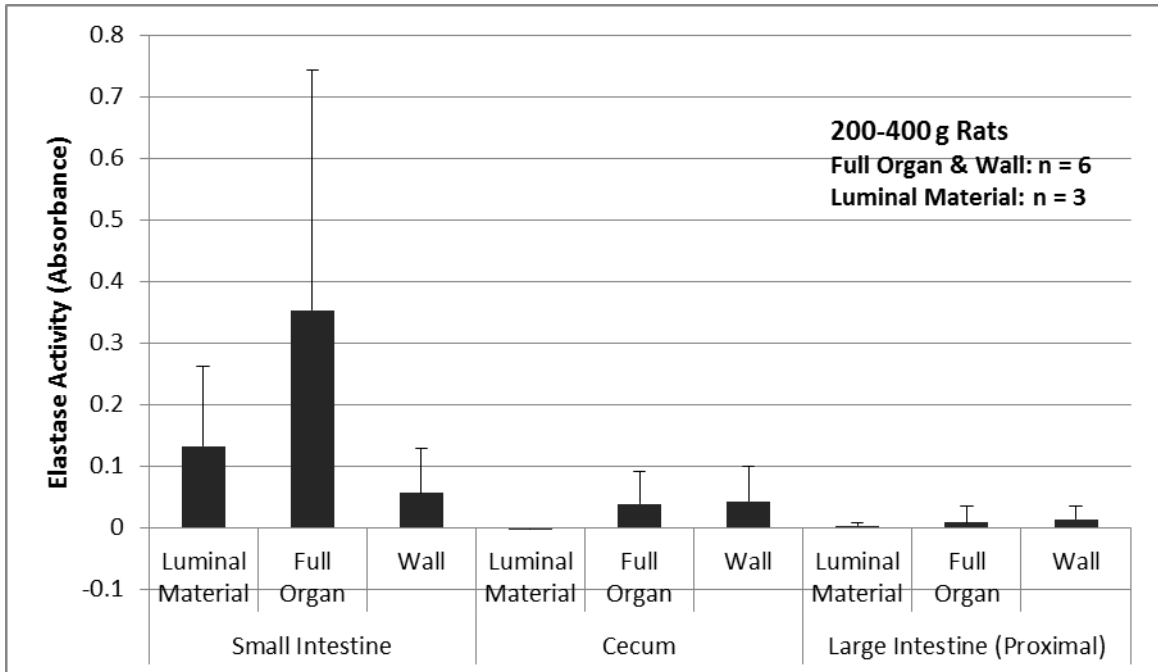


**Figure 2.5:** Average elastase activity at 75 minutes based on absorbance measurements. There is very high variation in the small intestine measurements for luminal material and full organ. No significant differences were found amongst the groups, although p-values between the complete organ versus cecum and full organ versus large intestine were close to 0.05.

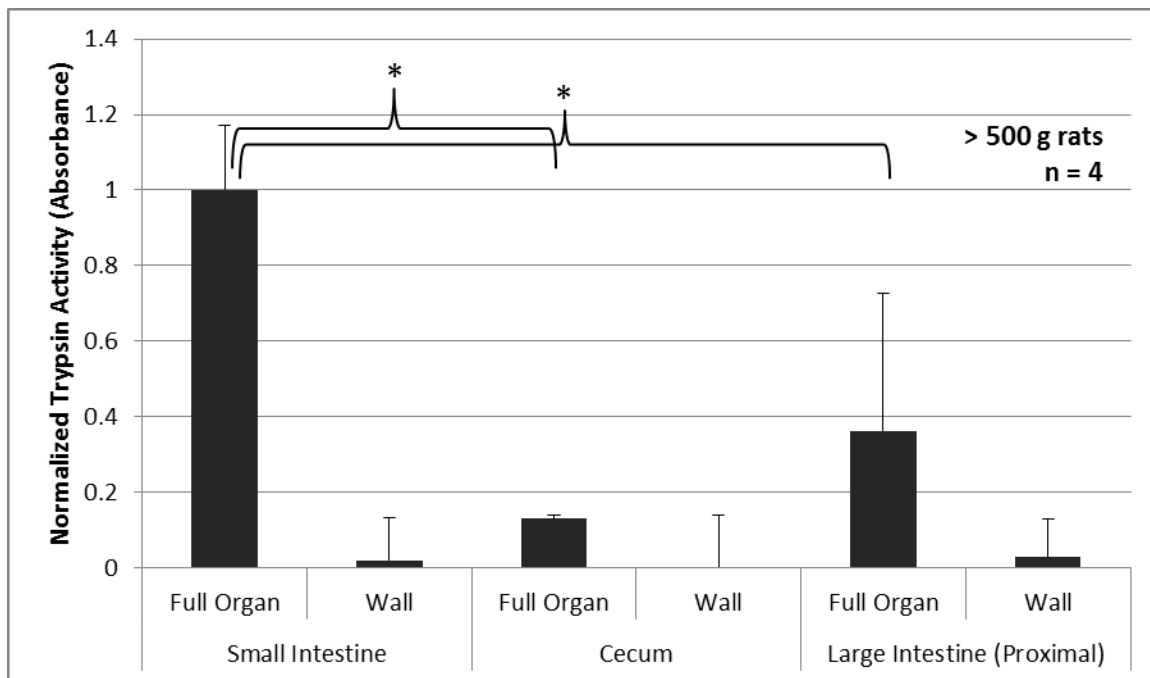


**Figure 2.6:** Average activity levels of trypsin at 75 minutes for animals greater than 500 g body weight. The same trends hold as with the younger animals; significant differences ( $p < 0.05$ ) were evident between the small intestine versus cecum, and small intestine versus large intestine. Luminal content data was not included in this graph.



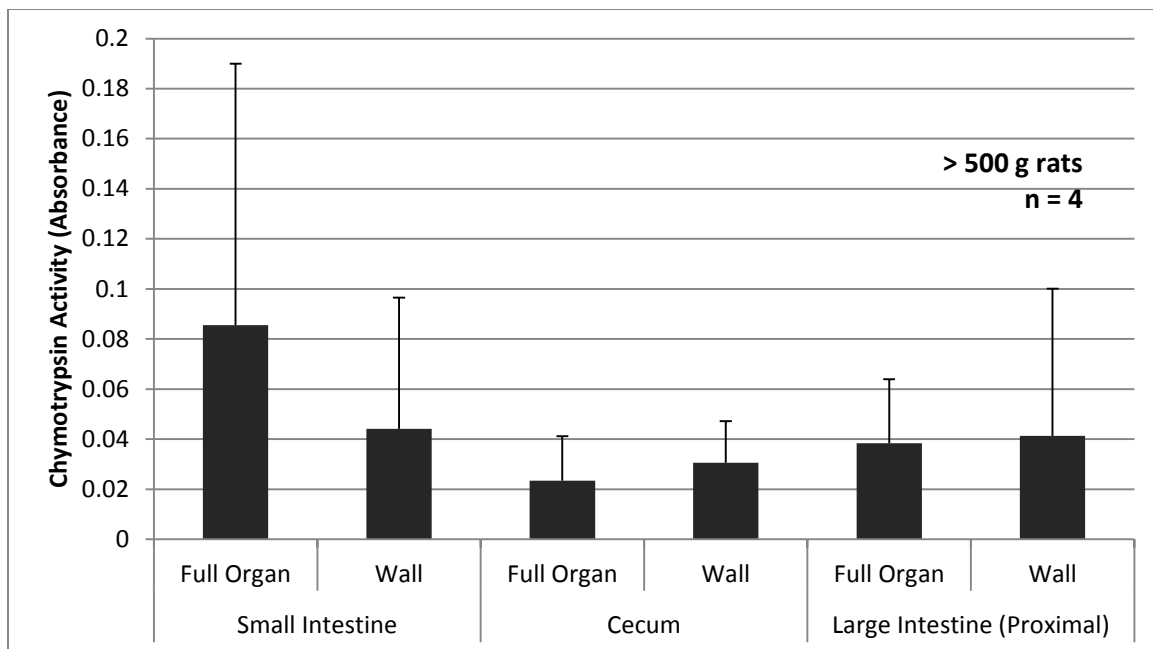


**Figure 2.7:** Average activity levels of chymotrypsin at 180 minutes for animals greater than 500 g. The same trends hold as with the younger animals; no significant differences were found between groups. Luminal content data was not included in this graph.

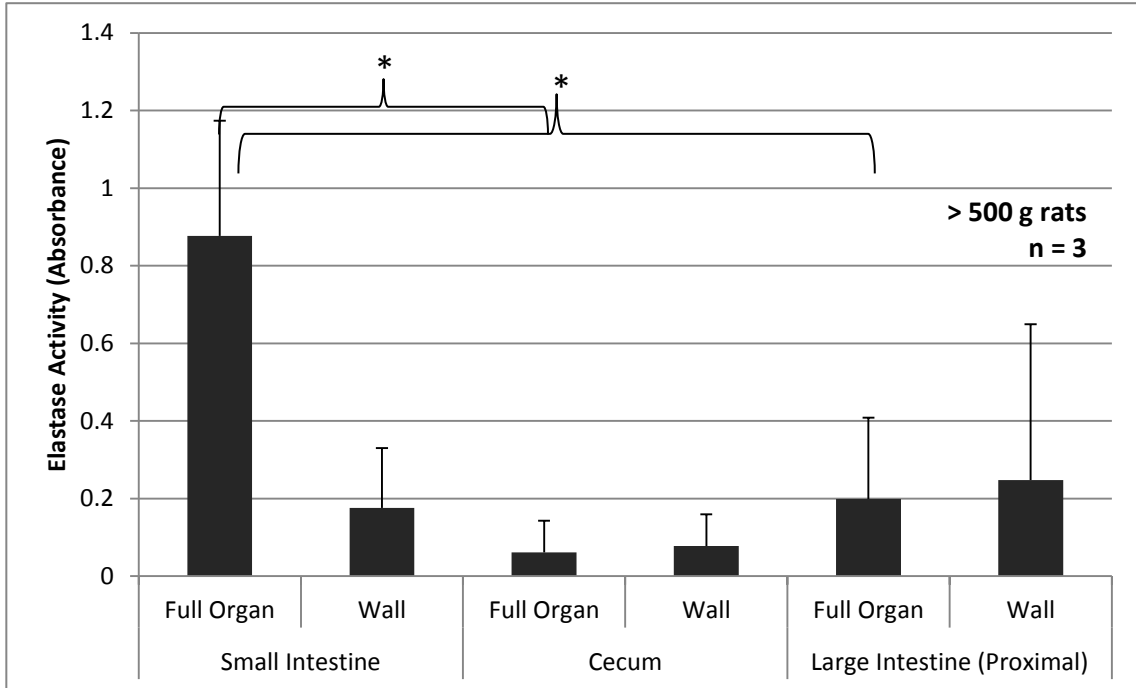


**Figure 2.8:** Average activity levels of elastase at 75 minutes for animals greater than 500 g. The same trends hold as with the younger animals; significant differences ( $p < 0.05$ ) were found between small intestine complete organ versus cecum and large intestine. Luminal content data was not included in this graph.

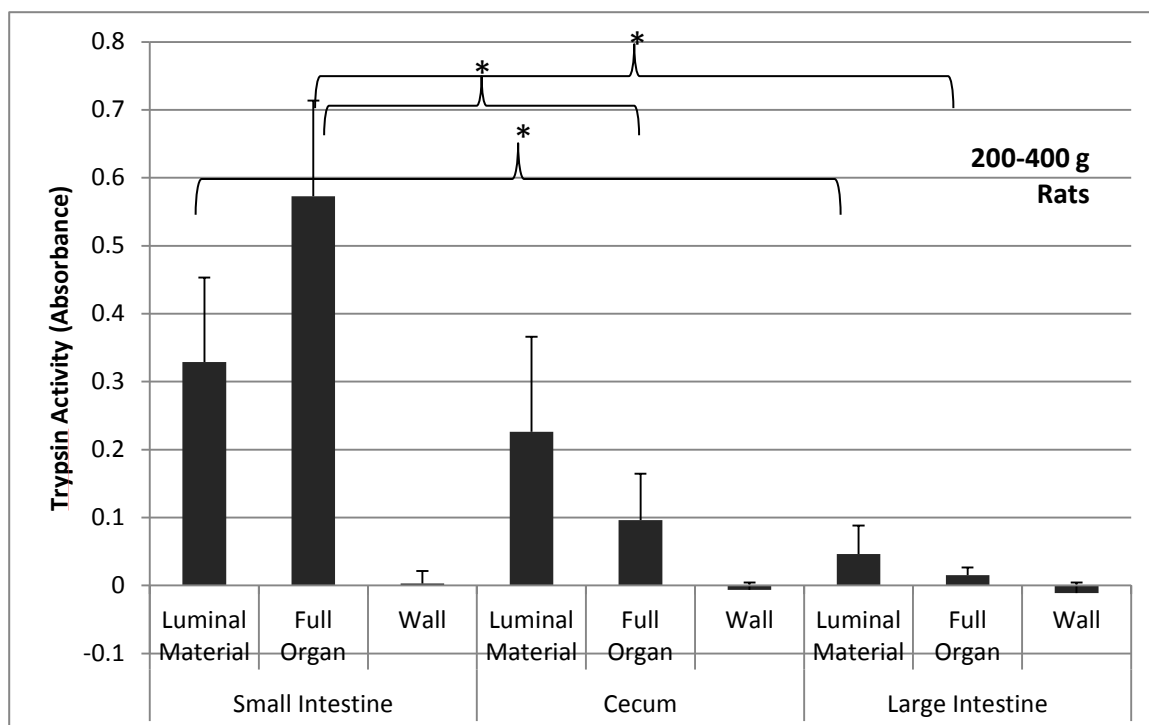


**Figure 2.9:** Average trypsin activity levels at 75 minutes for animals between 200 to 400 g in weight. The difference between these groups versus those in Figure 2.3 is the fact that the large intestine and wall samples were harvested about 2-4 cm from the end of the cecum as opposed to the junction; significant differences ( $p < 0.05$ ) were found between the small intestine versus cecum, and small intestine versus large intestine. There was also a significant difference between the activity in the luminal content of the small intestine versus that of the distal end of the large intestine, where the food is a solid pellet.

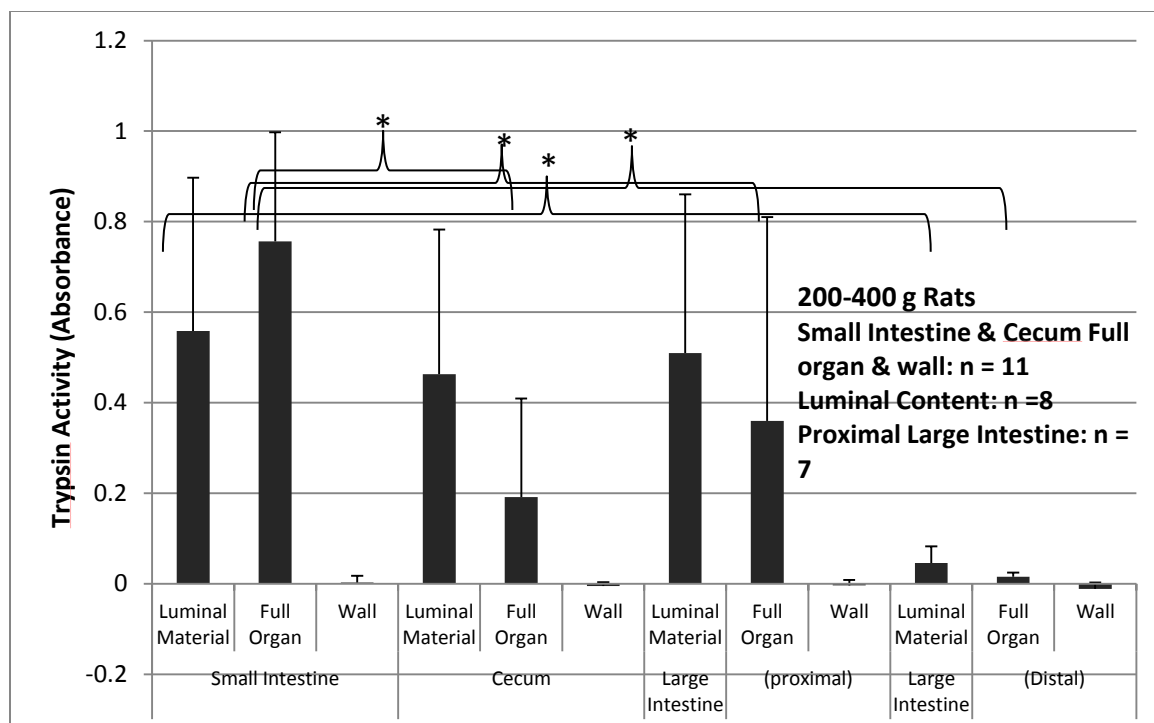


**Figure 2.10:** Average trypsin activity levels at 75 minutes for animals between 200 to 400 g in weight. As with Figure 2.09, the large intestine and wall samples were harvested about 2-4 cm from the end of the cecum as opposed to the junction; significant differences ( $p < 0.05$ ) were found between the small intestine versus cecum, small intestine versus large intestine, and the luminal content of the small intestine versus that in the distal end of the large intestine.

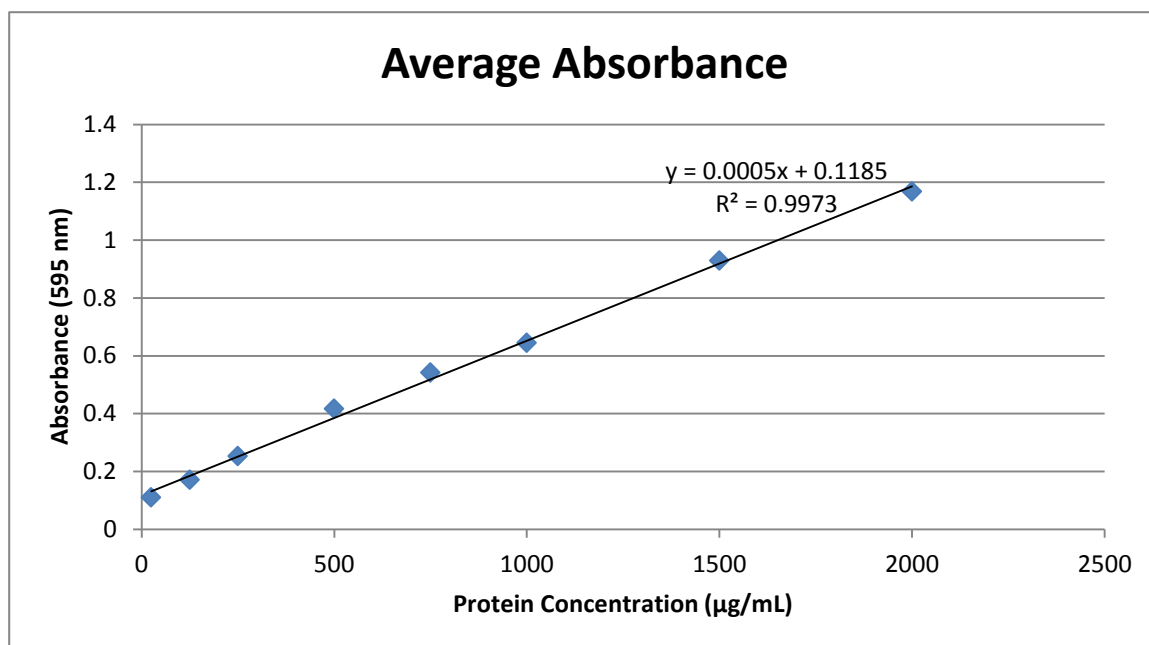


**Figure 2.11:** A curve of absorbance at 595 nm versus protein concentration in  $\mu\text{g/mL}$  using a BCA assay. The data are linear, and the resulting equation of the curve was used to determine protein concentrations of nine intestinal wall homogenates (small intestine, cecum, and large intestine, as well as their associated wall and luminal content) for three animals.

**Table 2.1:** Protein concentrations determined by BCA assay for nine sets of intestinal homogenate samples corresponding to three animals. Abbreviations are as follows; SI: small intestine, Lum: luminal content, Cec = cecum, and LI = large intestine.

Date (2012)	Undiluted Protein Concentration (mg/mL)	
24-Apr	SI	5.5556
	SI Wall	6.8188
	SI Lum	3.7836
	Cec	3.6328
	Cec Wall	3.9636
	Cec Lum	1.6972
	LI	2.4464
	LI Wall	3.4564
	LI Lum	2.8488
26-Apr	SI	4.6676
	SI Wall	5.2552
	SI Lum	1.4108
	Cec	4.012
	Cec Wall	3.2088
	Cec Lum	2.0304
	LI	8.5076
	LI Wall	4.2204
	LI Lum	1.7636
25-Oct	SI	2.9076
	SI Wall	6.4844
	SI Lum	1.3368
	Cec	5.9384
	Cec Wall	4.056
	Cec Lum	0.1676
	LI	5.4708
	LI Wall	0.1676
	LI Lum	1.0656

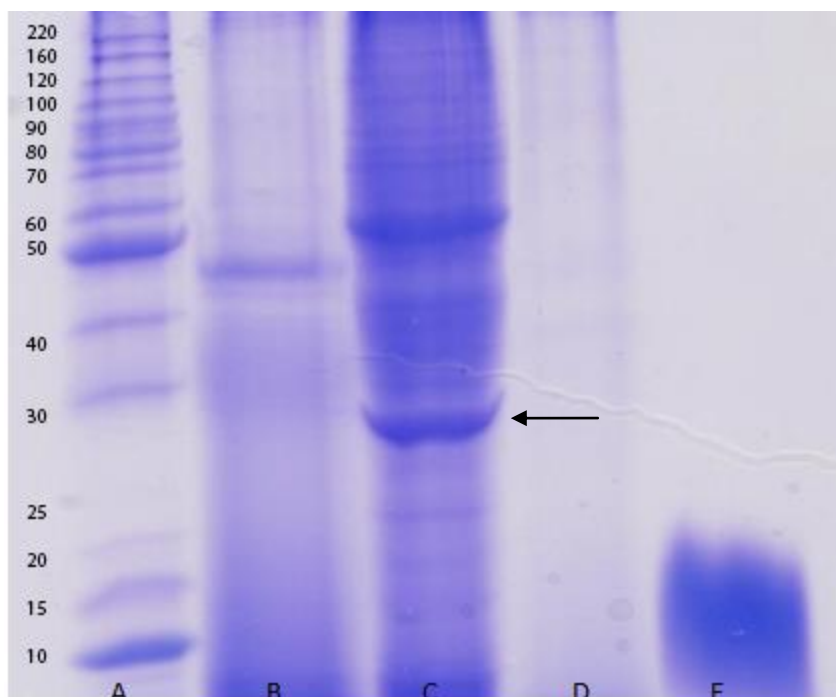


**Figure 2.12:** A 15% substrate-less gel with samples of intestinal wall homogenate (diluted 1:1) stained in 0.025% Coomassie Blue. **A:** protein ladder; **B:** small intestinal homogenate; **C:** cecal wall homogenate; **D:** large intestinal wall homogenate; and **E:** undiluted aprotinin (1.4 mg/mL). The bottom dark bands are remnants of the bromophenol blue dye front. The arrow indicates a band between 25 to 30 kDa that corresponds to the suspected trypsin inhibitor, based on reverse zymography. Protein concentrations were not normalized for each homogenate sample.

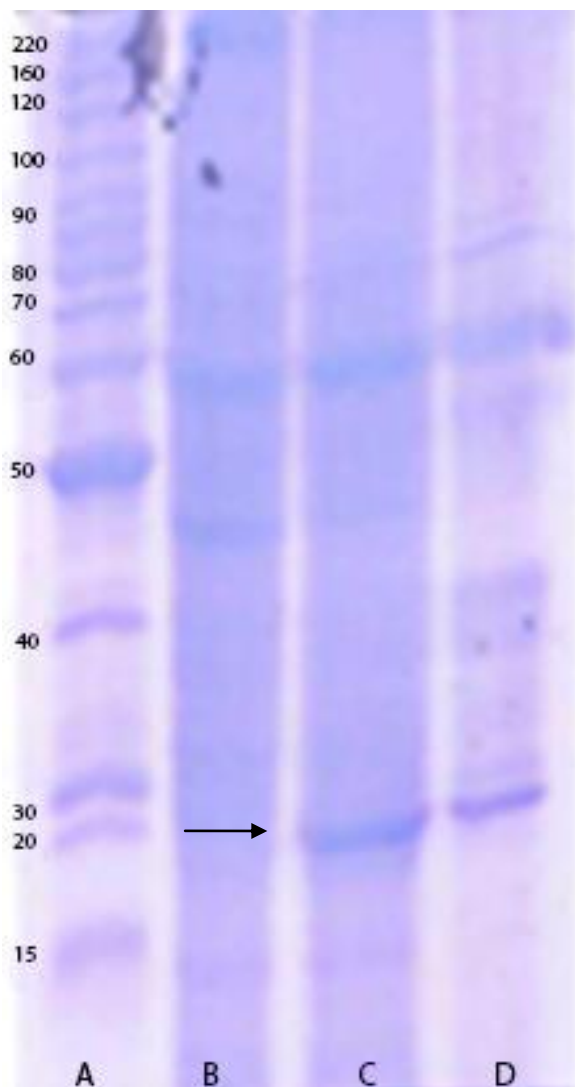


**Figure 2.13:** A 12% substrate-less gel with samples of intestinal wall homogenate (diluted 1:1) stained in 0.025% Coomassie Blue. **A:** protein ladder; **B:** small intestinal homogenate; **C:** cecal wall homogenate; and **D:** large intestinal wall homogenate. The arrow indicates a band between 25 to 30 kDa that corresponds to the suspected trypsin inhibitor, based on reverse zymography. Protein concentrations were not normalized for each homogenate sample.



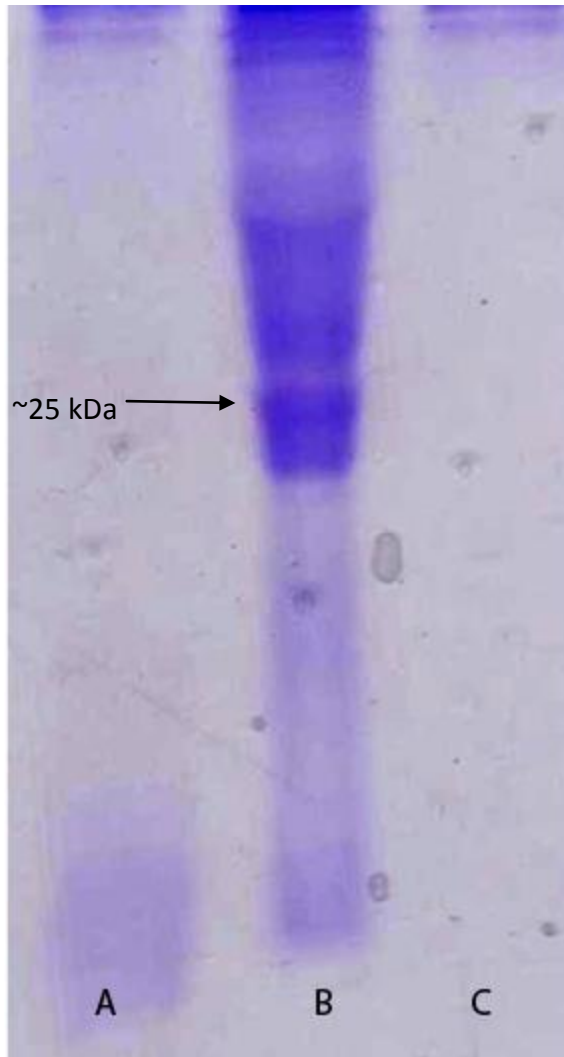


**Figure 2.14:** Image of a reverse zymogram with homogenates diluted 1:1. **A:** cecum (full organ) homogenate; **B:** cecal wall homogenate; and **C:** cecal luminal content homogenate. There is a noticeable Coomassie-stained band at the center of the gel corresponding to a ~25 kDa band, in Figure 2.11. Other activity bands exist, but this specific band is unique to the cecal wall homogenate and is not present in the small intestinal wall homogenate, which shows higher trypsin activity than the cecal wall. Protein concentrations were not normalized for each homogenate sample.

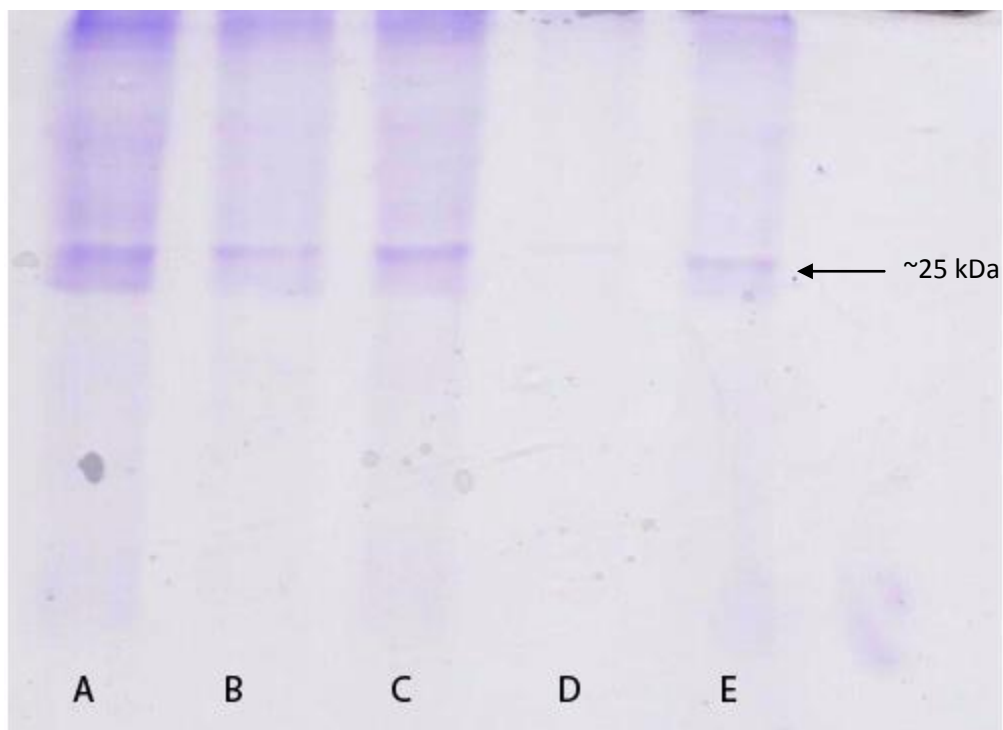


**Figure 2.15:** Image of a reverse zymogram using five different dilutions of cecal wall homogenate (derived from the same homogenate). In ratio of dilution: **A:** 1:1, **B:** 1:2, **C:** 1:3, **D:** 1:4 (oldest prepared sample; the other samples were prepared weeks afterward on the same day), and **E:** 1:5. Using this zymogram, it was determined that a 1:1 dilution ratio was ideal for optimal band visualization following a 16-hour overnight incubation. The arrow points to the position of an inhibitor (protein) based on the prominent band stained by Coomassie blue (Figure 2.11 arrows).

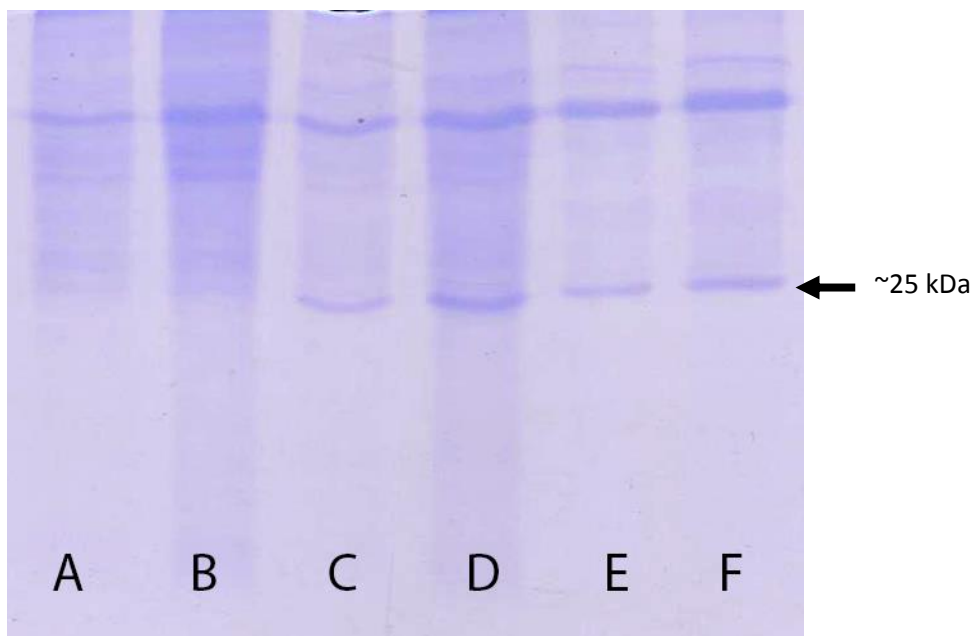


**Figure 2.16:** A reverse zymogram of wall homogenates of equal protein concentration by order of magnitude diluted 1:1. The lanes and amount of protein placed into the lanes are: **A:** small intestine wall – 10  $\mu\text{g}$ ; **B:** small intestine wall – 20  $\mu\text{g}$ ; **C:** cecal wall – 10  $\mu\text{g}$ ; **D:** cecal wall – 20  $\mu\text{g}$ ; **E:** large intestine wall – 10  $\mu\text{g}$ ; **F:** large intestine wall – 20  $\mu\text{g}$  (in well). The arrow indicates a band in the 25 kDa range for the cecal wall and large intestinal wall homogenates.

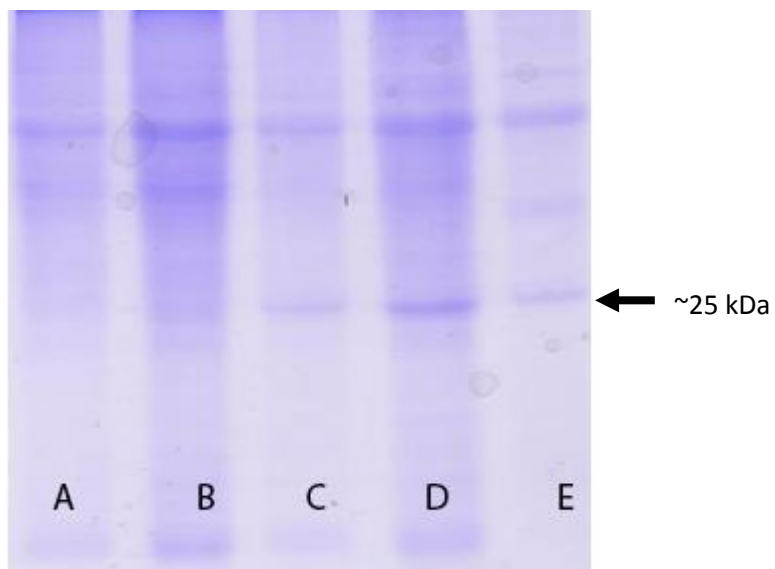


**Figure 2.17:** A reverse zymogram of wall homogenates (at equal protein concentration by order of magnitude) diluted 1:1. The lanes and amount of protein placed into the lanes are: **A:** small intestine wall – 10 µg; **B:** small intestine wall – 20 µg; **C:** cecal wall – 10 µg; **D:** cecal wall – 20 µg; **E:** large intestine wall – 10 µg (in well). The arrow indicates a band in the 25 kDa range for both the cecal wall and large intestine wall samples.

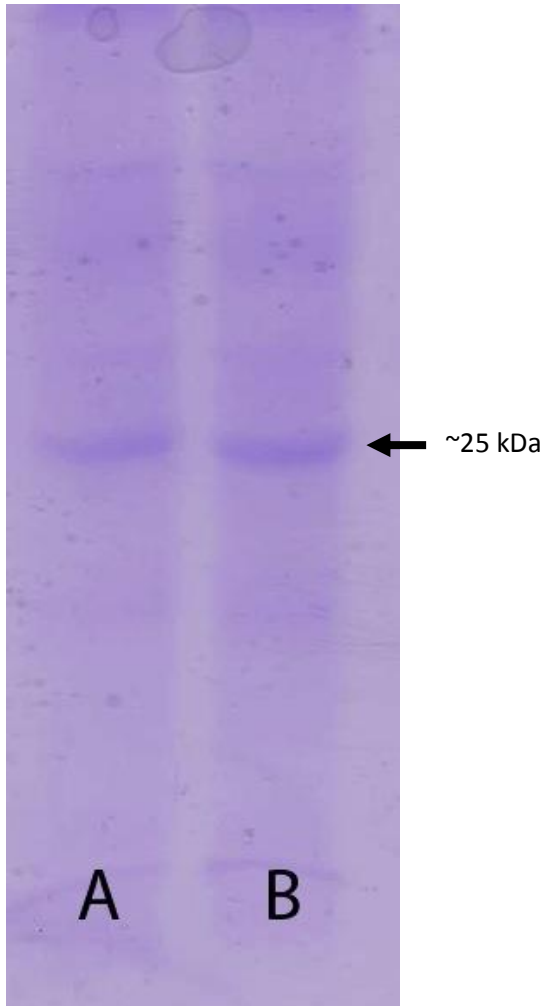


**Figure 2.18:** A reverse zymogram of two cecal wall homogenates (20  $\mu\text{g}$  per well) incubated overnight in 10x the amount of trypsin normally used in the developing buffer. Both **A** and **B**, with molecular weights of  $\sim 25$  kDa, have the same protein concentration.

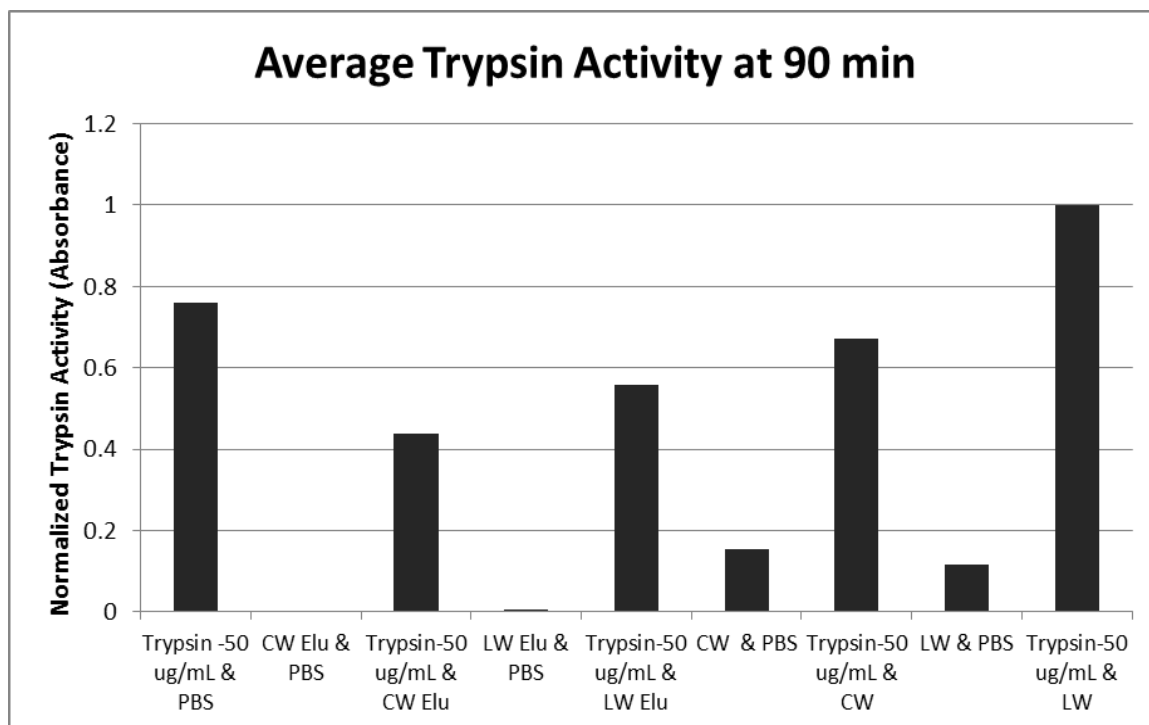


**Figure 2.19:** A histogram of the average trypsin activity at 75 minutes in samples of intestinal wall homogenates mixed with an equal volume of trypsin, as well as trypsin and wall homogenate controls from a pilot study. Pilot studies showed that 50  $\mu\text{g}/\text{mL}$  of trypsin offered the best absorbance curve, and smaller volumes offered insufficient absorbance for quantitative measurements. A decrease of activity by about 50% was noted when samples of cecal wall homogenate eluted from the estimated 25 kDa band location (CW Elu) was mixed with trypsin. Only a decrease of about 30% was noted for a large intestinal wall homogenate mix (LW Elu). Unpurified samples of cecal wall (CW) did not show much reduction when compared to eluted cecal wall, while unpurified samples of large intestinal wall (LW) actually increased activity when mixed with trypsin.

**Table 2.2:** Proteins found in a sample of HPLC-purified cecal wall homogenate. The name of the protein is listed on the left column, while the name of the species is listed on the right column. The immunoglobulin heavy chain (gamma polypeptide) is highlighted due to its potential to act as, or contain, the unknown inhibitor of interest.

Name	Species
keratin 10 [Rattus norvegicus]	Rattus norvegicus
keratin 1 [Rattus norvegicus]	Rattus norvegicus
RecName: Full=Trypsin; Flags: Precursor	PIG
keratin	
keratin 2 [Rattus norvegicus]	Rattus norvegicus
keratin 5 [Rattus norvegicus]	Rattus norvegicus
Keratin, type II cytoskeletal 6B (Cytokeratin-6B) (CK 6B) (K6b keratin)	HUMAN
beta-globin [Rattus norvegicus]	Rattus norvegicus
beta globin minor [Rattus norvegicus]	Rattus norvegicus
PREDICTED: similar to Hemoglobin beta-2 subunit (Hemoglobin beta-2 chain) (Beta-2-globin) (Hemoglobin beta chain, minor-form) [Rattus norvegicus]	Rattus norvegicus
<b>Immunoglobulin heavy chain (gamma polypeptide) [Rattus norvegicus]</b>	Rattus norvegicus
development and differentiation enhancing factor 2 [Rattus norvegicus]	Rattus norvegicus
Keratin, type II cytoskeletal 6A (Cytokeratin-6A) (CK 6A) (K6a keratin) (Cytokeratin-6D) (CK 6D) (Allergen Hom s 5)	HUMAN
Keratin, type II cytoskeletal 6B (Cytokeratin-6B) (CK 6B) (K6b keratin)	HUMAN
hypothetical protein LOC683313 [Rattus norvegicus]	Rattus norvegicus
PREDICTED: similar to keratin complex 2, basic, gene 6a isoform 2 [Rattus norvegicus]	Rattus norvegicus
PREDICTED: similar to keratin complex 2, basic, gene 6a isoform 1 [Rattus norvegicus]	Rattus norvegicus
TAO kinase 3 [Rattus norvegicus]	Rattus norvegicus

## Ch 2.3 Discussion

### Ch 2.3.1 Colorimetric Plate Assay

There have been relatively few studies that have focused on proteolytic activity in different areas of the gastrointestinal tract.<sup>64, 65, 66, 67</sup> One such study<sup>64</sup> focused on the brush border membrane (BBM) and luminal enzymes from the small intestine and colon of guinea pigs, in which peptide and protein degradation, particularly that of insulin and insulin B-chain, were observed. The *in vitro* study found that insulin and insulin B-chain degradation occurred relatively quickly in the small intestine as compared to the colon.<sup>68</sup> Although luminal pellets did show substantial activity<sup>68</sup>, it could be from either extracellular proteolytic activity or cell lysis.<sup>69</sup> Another study found that some enzymes, such as endopeptidase-2, are more active in the duodenum than in the ileum, while others—such as carboxypeptidase P and aminopeptidase P—show similar activity in both the ileum and duodenum of rats.<sup>70</sup> Ultimately, the BBM and luminal content study, along with previous research performed by the same group, concluded that polymeric substrates and small oligopeptides degraded more quickly in the presence of brush border and luminal enzymes in the small intestine as opposed to the colon, where degradation rate was found to be minimal or negligible.<sup>71</sup> Could this be a correlation to a greater presence of digestive enzymes in the small intestine as opposed to the large intestine?

The results of the serine protease activity assays in this study revealed that in the case of trypsin activity, there was a notable reduction of activity in the full organs of the



cecum and the large intestine as compared to the full organ of the small intestine (**Figures 2.3, 2.6, 2.9, and 2.10**). Intestinal wall homogenates for these three organs had little to no protease activity, while activity in the luminal content of the homogenates was typically similar to that of the full organ. In contrast, the case of the solid pellet-like luminal content in the distal end of the large intestine (colon) exhibited a notable decrease in trypsin activity (**Figures 2.9 and 2.10**). These results suggest that a serine protease inhibitor may be present in or secreted by the cecal wall and possibly also in the large intestinal wall, resulting in the attenuation of trypsin activity during the transition from the ileum to the cecum. Furthermore, by the time the luminal material has transitioned into the colon and has been dehydrated, forming more solid pellets as opposed to more liquid food waste, trypsin activity was greatly reduced as compared to when food was present in the small intestine.

The results of the chymotrypsin and elastase activity assays yielded no consistent or significant reduction in activity between the small intestine and large intestine homogenates. As such, my experiments were designed to determine potential inhibitor activity focused on trypsin.

The results of these assays are in contrast to the previous studies of the GI colon and large intestine, in which the degradation rate of various enzymes was found to be minimal in comparison to that of the small intestine.<sup>71</sup> However, it can be argued that slower degradation rate does not necessarily mean that a gradient for serine protease activity does not exist. A recent study<sup>72</sup> revealed that at that serine protease activity, measured as a function of liberated tyrosine, stays relatively constant during the transition

of the ileum to the ileocecal junction, thereby suggesting that there is no marked decrease in protease gradient down the length of the intestine. Given that trypsin activity decreased markedly from ileum to cecum, a different mechanism than simple enzymatic degradation appears to be at play, at least in the case of this particular digestive enzyme. Hence we can most likely rule out such marked enzymatic degradation of trypsin in the transition from the ileum to the colon.

### **Ch 2.3.2 Reverse Zymography Results**

The results of the reverse zymograms from **Figure 2.14** to **Figure 2.20** suggest the existence of a trypsin protease inhibitor in the cecal wall homogenate, and possibly in the large intestinal wall. The band that appeared around 25 to 30 kDa in the cecal wall homogenate consistently appeared in each of the 26 successful reverse zymograms, often in lieu of other prominent bands that exist in the SDS PAGE gel (such as the band between 50 to 60 kDa in molecular weight). The large intestinal wall also showed a fainter band at approximately the same molecular weight range as the cecal wall homogenate when protein concentration is normalized, as was the case for the gels in **Figures 2.18** to **2.20**.

In many of the reverse zymograms, a band around 50 to 60 kDa in molecular weight was visible, but this band appeared to be present in all intestinal wall homogenate samples at the same concentration. Hence, we suspect that this band could not have served a role as an inhibitor. Subsequent experiments using a higher concentration of trypsin in the developing buffer revealed that the band in question was digested by the trypsin, while the 25 to 30 kDa band in the cecal wall still remained (**Figure 2.20**). These

results are consistent with the hypothesis that a serine protease inhibitor is present in the cecal wall of the rat, resulting in the attenuation of trypsin activity as detected in plate zymography.

### **Ch 2.3.3 High-Performance Liquid Chromatography and Mass Spectroscopy Results**

The plate zymography experiments in which cecal wall and large intestinal wall homogenates, both unpurified and eluted, were mixed in equal volumes with trypsin at a concentration of 50  $\mu\text{g}/\text{mL}$  (**Figure 2.21**), revealed that there is a 50% decrease in activity. In comparison, there was a 30% reduction in activity when eluted large intestinal wall homogenate was mixed in equal volumes with 50  $\mu\text{g}/\text{mL}$  trypsin. In contrast, un-eluted homogenates of cecal wall showed minimal attenuation of activity, while un-eluted large intestinal wall homogenate revealed an increase. While neither of the eluted homogenate results is considered statistically significant, the results are interesting and deserve further study.

The results of mass spectroscopy of the cecal wall homogenates reveal a number of proteins that can be found in the cecal wall (**Table 2.2**). Among potential candidates, only the immunoglobulin heavy chain (gamma peptide) appears viable as a potential inhibitor of trypsin due to studies with antibodies acting as protease inhibitors,<sup>55,58</sup> including the ability to engineer Kunitz domain inhibitors from camelid heavy chains.<sup>56,57</sup> Future studies should be done to determine whether this immunoglobulin heavy chain can actually act as a trypsin inhibitor.

Compared to other areas of the GI tract, the large intestine and colon are better locations for mucoadhesion, the adhesion between a surface to a mucosal layer.<sup>73</sup> Mucoadhesives bind more strongly to the mucus layer than the mucin layers.<sup>74</sup> Less mucus secretion in the GI tract organ provides better mucoadhesion.<sup>73</sup> Study of the mucus gel thickness and turnover rate (based on secretion) in the stomach, proximal jejunum, cecum, and proximal colon of the rat indicates that the cecum and colon have the lowest turnover rates.<sup>73</sup> In addition, there is a decrease in mucus secretion rate in the cecum as opposed to the jejunum.<sup>73</sup> Adherence of various copolymers with specific binding properties is greater in the mucosa of the colon than in the small intestine of the rat<sup>74</sup>, at least in enterocytes measured within the mucosa layer as opposed to isolated cells.<sup>75</sup> Could the improved mucoadhesion in the cecum and colon allow for more enzymes such as a trypsin inhibitor, to be better retained in this area of the GI tract as opposed to the small intestine and stomach?

Such studies, in addition to those measuring proteolytic activity in the intestinal tract<sup>76</sup>, suggest that net proteolytic activity is indeed lower in the large bowel than in the small intestine, consistent with my own results. What is unclear is whether the cecum and colon have enzymes that inhibit the activity of digestive enzyme inhibitors that block the activity of digestive enzymes in the large intestine. When combining the findings that enzymatic degradation rate in the colon is lower than in the small intestine<sup>71</sup>, thus making enzymatic degradation unlikely, the present study suggests that an unidentified inhibitor may in fact be secreted in the cecum and possibly the large intestine. Further studies are needed in order to isolate and determine the identity of this unknown trypsin inhibitor.

## Ch 2.4 Conclusion

This study suggests that proteolytic activity of serine proteases, trypsin in particular, is reduced during the transition from the small intestine to the colon via the ileocecal junction. The decrease is most notable between the full organ (wall and luminal content) of the small intestine versus that of the cecum, and versus that of the distal end of the colon. This phenomenon would suggest that either an inhibitor of trypsin is present in or secreted by the cecal wall, or enzymatic degradation of trypsin occurs down the length of the intestine. The literature suggests that the latter is not the case, and subsequent reverse zymography studies and purification via protein elution suggest that an unidentified inhibitor may be responsible for the attenuation in trypsin activity in the large intestine. The findings thus support our hypothesis that serine protease activity is reduced in the large intestine as a way for the colon to protect against potential autodigestion and generation of inflammatory mediators in the large bowel, where digested food is dehydrated and maintained for longer periods than in the small bowel.

## References

1. Vanlaere, I, C Libert. Matrix Metalloproteinases as Drug Targets in Infections Caused by Gram-Negative Bacteria in Septic Shock. *Clinical Microbiology Reviews* **22**: 224-239, 2009.
2. Angus, DC, WT Linde-Zwirble, J Lidicker, G Clermont, J Carcillo, and MR Pinsky. Epidemiology of severe sepsis in the United States: analysis of incidence, outcome, and associated costs of care. *Crit. Care Med.* **29**: 1303–1310, 2001.
3. Schmid-Schönbein GW, Hugli TE, Kistler EB, Sofianos A, and Mitsuoka H. Pancreatic enzymes and microvascular cell activation in multiorgan failure. *Microcirculation* **8**: 5–14, 2001.
4. Schmid-Schönbein GW and Hugli TE. A New Hypothesis for Microvascular Inflammation in Shock and Multiorgan Failure: Self-Digestion by Pancreatic Enzymes. *Microcirculation* **12**: 71-82, 2005.
5. Yao YM, Redl H, Bahrami S, Schlag G. The Inflammatory basis of trauma/shock-associated multiple organ failure. *Inflamm Res* **47**: 201-210, 1998.
6. Mitsuoka H & GW Schmid-Schönbein. Mechanisms For Blockade of *In Vivo* Activator Production in the Ischemic Intestine and Multi-Organ Failure. *Shock* **14**: 522-527, 2000.
7. Cheatham, ML, Block, EFJ, Smith, HG, Promes, JT Shock: An Overview. In *Intensive Care Medicine* 1761-1778 (Lippincott-Raven, Philadelphia, 2003).
8. Deitch, EA. Multiple organ failure. Pathophysiology and potential future therapy. *Ann Surg* **216**: 117-34, 1992.
9. Acosta, JA, Hoyt DB, Schmid-Schönbein GW, Hugli TE, Anjaria DJ, Frankel DA, Coimbra R. Intraluminal Pancreatic Serine Protease Activity, Mucosal Permeability, and Shock: A Review. *Shock* **26**: 3-9, 2006.
10. Penn AH, Hugli TE, Schmid-Schönbein GW. Pancreatic Enzymes Generate Cytotoxic Mediators in the Intestine. *Shock* **27**: 296-304, 2007.
11. Rothaman S, Liebow C, Isenman L: Conservation of digestive enzymes. *Physiol Rev* **82**:1-18, 2002.
12. Malinoski, D. J., Barrios, C., Kim, H. D., Acosta, J. A., Schmid-Schönbein, G. W., Hugli, T. E., Coimbra, R., Hoyt, D. B., Role of pancreatic enzymes in the

- development of multiple organ failure after shock. *J. Organ Dysfunction*, **4**, 161–167, 2008.
13. Mitsuoka, H., Kistler, E.B., Schmid-Schönbein, G.W.: Generation of in vivo activating factors in the ischemic intestine by pancreatic enzymes. *Proc. Nat. Acad. Sci. U.S.A.*, *97*:1772-1777, 2000.
  14. Kistler, E.B., Hugli, T.E., Schmid-Schönbein, G.W.: The pancreas as a source of cardiovascular cell activating factors. *Microcirculation*, *7*:183-192, 2000.
  15. Rosario HS, Waldo SW, Becker SA, Schmid-Schönbein GW: Pancreatic trypsin increases matrix metalloproteinase Y9 accumulation and activation during acute intestinal ischemia-reperfusion in the rat. *Am J Pathol* *164*: 1707Y1716, 2004.
  16. Mitsuoka, H., Kistler, E. B., Schmid-Schönbein, G.W.: Protease inhibition in the intestinal lumen: Attenuation of systemic inflammation and early indicators of multiple organ failure in shock. *Shock* *17*:205-209, 2002.
  17. Fitzal, F., DeLano, F.A., Young, C., Rosario, H.S, Schmid-Schönbein, G.W.: Pancreatic protease inhibition during shock attenuates cell activation and peripheral inflammation. *J. Vasc. Res.*, *39*:320-329, 2002.
  18. Lefer AM. Role of a myocardial depressant factor in the pathogenesis of circulatory shock. *Fed Proc*, *29*:1836–1847, 1970.
  19. McCord, JM. Oxygen-derived free radicals in postischemic tissue injury. *N Engl J Med* **312**, 159-63 (1985).
  20. Waldo, SW, Rosario, HS, Penn, AH, Schmid-Schonbein, GW. Pancreatic digestive enzymes are potent generators of mediators for leukocyte activation and mortality. *Shock* **20**, 138-43, 2003.
  21. Wiedow, O., Meyer-Hoffert, U. Neutrophil serine proteases: potential key regulators of cell signaling during inflammation. *Journal of Internal Medicine* *257*, 319-28, 2005.
  22. Heikius, B., Niemela, S., Lehtola, J., Karttunen, T. J., Elevated Pancreatic Enzymes in inflammatory bowel disease are associated with extensive disease. *Am. J. Gastroenterol.*, *94*, 1062–1069, 1999.
  23. DeLano, F. A., Schmid- Schönbein, G. W., Proteinase Activity and Receptor Cleavage: Mechanism for Insulin Resistance in the Spontaneously Hypertensive Rat. *Hypertension* 2008, *52*, 415–423.

24. Lee, S. W., Song, K. E., Shin, D. S., Ahn, S. M., Ha, E. S., Kim, D. J., Nam, M. S., Lee, K. W., Alterations in peripheral blood levels of TIMP-1, MMP-2, and MMP-9 in patients with type-2 diabetes. *Diabetes Res. Clin. Pract.* **69**, 175–179, 2005.
25. Deitch E, DaZhong X, Kaiser VL. Role of the gut in the development of injury- and shock induced SIRS and MODS: the gut-lymph hypothesis, a review. *Frontiers in Bioscience*, **11**, 520-528, 2006.
26. Deitch, E.A., Shi, H.P., Lu Q., Feteova, E., Xu, D.Z. Serine Proteases are Involved in the Pathogenesis of Trauma-Hemorrhagic Shock-Induced Gut and Lung Injury
27. Fitzal, F., DeLano, F.A., Young, C., Schmid-Schonbein, G.W. Improvement in early symptoms of shock by delayed intestinal protease inhibition. *Arch Surg* 139, 1008-16, 2004.
28. Caldwell-Kenkel JC, Currin RT, Tanaka Y, Thurman RG, Lemasters JJ. Reperfusion injury to endothelial cells following cold storage of rat liver. *Hepatology*. 10, 292–299, 1989.
29. Jaeschke, H., Lemasters, J.J. Apoptosis versus Oncotic Necrosis in Hepatic Ischemia Reperfusion Injury. *Gastroenterology* 125. 1246-57, 2003.
30. Mura, M., Andrade CF, Han B, Seth R, Zhang Y, Bai, XH, Waddell, TK, Hwang, D, Keshavjee, S, Liu M. Intestinal ischemia-reperfusion-induced acute lung injury and oncotic cell death in multiple organs. *Shock* 28, 227-38, 2007.
31. Lichtman S.N., Lemasters J.J. Role of cytokines and cytokine-producing cells in reperfusion injury to the liver. *Semin Liver Dis* 19, 171–187, 1999.
32. Jaeschke H, Woolbright BL. Current Strategies to minimize hepatic ischemia-reperfusion injury by targeting reactive oxygen species. *Transplantation Reviews* 26, 103-114, 2012.
33. Nishimura Y, Lemasters JJ. Glycine blocks opening of a death channel in cultured hepatic sinusoidal endothelial cells during chemical hypoxia. *Cell Death Differ* 2001;8:850–858.
34. Nieminen AL, Gores GJ, Wray BE, Tanaka Y, Herman B, Lemasters JJ. Calcium dependence of bleb formation and cell death in hepatocytes. *Cell Calcium* 9:237–246, 1988.
35. Zahrebelski G, Nieminen AL, Al-Ghoul K, Qian T, Herman B, Lemasters JJ. Progression of subcellular changes during chemical hypoxia to cultured rat hepatocytes: a laser scanning confocal microscopic study. *Hepatology* 21, 1361–1372, 1995.



36. Iqbal T, Rabnawaz AI, Tahir F, Zaman S. A Meta analysis of history and functions of vermiform appendix. *Pak J Surg* 27, 316-320, 2011.
37. Borley NR. Vermiform appendix, In: Standing S, Ellis H, Healy JC, Johnson D, Williams A, Collins P, editors. *Gray's anatomy: the anatomical basis of clinical practice*. 39th ed. Edinburgh: Elsevier Churchill Livingstone; 1189- 90, 2005.
38. Sadler, T.W.: *Langman's Medical embryology*. 10th Ed; Williams and Wilkins. Baltimor. 221-2, 2006.
39. Seal A. Appendicitis: a historical review. *Canadian J. of Surg.*, 24, 427, 1981.
40. Way, L.W., *Current Surgical Diagnosis and Treatment*, Lange. Seventh Edition, 1985.
41. Chadwick. V.S. and Phillips. S., *Small Intestine B.I.M.R. Gastroenterology* 2. Butterworth. 1982.
42. Alexander-Williams. I. and Binder. H.I., *Large Intestine B.I.M.R. Gastroenterology* 3. Butt erworth. 1983.
43. Subbaswamy, SG. Patterns of Mucin Secretion in human intestinal mucosa. *J. Anat.* **108**, 291-293, 1969.
44. Doe. W. Immunology of the gastrointestinal tract. *Medicine International*. 1986..2:1044.
45. Sussdorf. D.M. and Draper. L.R... Antibodies in rabbits after irradiation; shielding the appendix. *J. of Infect. Dis.*, 1956, 99:129
46. Archer. O.K., Sutherland. D.R., Good. R.A. The appendix in rabbits after neonatal thymectomy. *Nature*. 2, 1963, 300:337
47. Guadalupe GT., Lee FY., Barden G.E., Cartun R., West A.B. Bacterial Translocation to Mesenteric Lymph Nodes Is Increased in Cirrhotic Rats With Ascites. *Gastroenterology*. 108, 1835-41, 1995.
48. Miyata S, Miyagi Y, Koshikawa N, Nagashima Y, Kato Y, Yasumitsu H, Hirahara F, Misugi K and Miyazaki K. Stimulation of cellular growth and adhesion to fibronectin and vitronectin in culture and tumorigenicity in nude mice by overexpression of trypsinogen in human gastric cancer cells. *Clin Exp Metastasis* **16**: 613–622, 1999.
49. Bernard-Perrone F, Carrere J, Renaud W, Moriscot C, Thoreux K, Bernard P, Servin A, Balas D and Senegas-Balas F. Pancreatic trypsinogen I expression during

- cell growth and differentiation of two human colon carcinoma cells. *Am J Physiol* **274**: G1077–1086, 1998.
50. Hedstrom J, Haglund C, Haapiainen R and Stenman UH. Serum trypsinogen-2 and trypsin-2-alpha(1)-antitrypsin complex in malignant and benign digestive-tract diseases. Preferential elevation in patients with cholangiocarcinomas. *Int J Cancer* **66**: 326–331,1996.
51. Ichikawa Y, Koshikawa N, Hasegawa S, Ishikawa T, Momiyama N, Kunizaki C, Takahashi M, Moriwaki Y, Akiyama H, Yamaoka H, Yanoma S, Tsuburaya A, Nagashima Y, Shimada H and Miyazaki K. Marked increase of trypsin(ogen) in serum of linitis plastica (gastric cancer, borrmann 4) patients [In Process Citation]. *Clin Cancer Res* **6**: 1385–1388, 2000.
52. Kennedy AR. Prevention of carcinogenesis by protease inhibitors. *Cancer Res* **54**: 1999s–2005s, 1994.
53. Kennedy AR. The Bowman-Birk inhibitor from soybeans as an anticarcinogenic agent. *Am J Clin Nutr* **68**: 1406s–1412s, 1998.
54. Darmoul, D, Marie JC, Devaud H, Gratio V, Laburthe M. Initiation of human colon cancer cell proliferation by trypsin-acting at protease-activated receptor-2. *British Journal of Cancer*. **85**, 772-779, 2001.
55. Gerber, F, Krummen M, Potgeter H, Roth A, Siffrin C, Spoendlin C. Practical aspects of fast reversed-phase high-performance liquid chromatography using 3µm particle packed columns and monolithic columns in pharmaceutical development and production working under current good manufacturing practice. *Journal of Chromatography A*. **1036**, 127-133, 2004.
56. Ganesan, R, Eigenbrot C, Kirchhofer D. Structural and mechanistic insight into how antibodies inhibit serine proteases. *Biochem J*. **430**, 179-189, 2010.
57. Radisky, ES, Koshland Jr, DE. A clogged gutter mechanism for protease inhibitors. *Proc. Natl. Acad. Sci. U.S.A.* **99**, 10316-10321, 2002.
58. Nixon, AE, Wood CR. Engineered protein inhibitors of proteases. *Curr. Opin. Drug Discovery Devel.* **9**, 261-268, 2006.
59. Martin, F, Volpari C, Steinkuhler C, Dimasi N, Brunetti M, Biasol G, Altamura S, Cortese R, De Francesco R, Sollazzo M. Affinity selection of a camelized V(H) domain antibody inhibitor of hepatitis C virus NS3 protease. *Protein Eng.* **10**, 607-614, 1977.

60. Dickinson, CD, Shobe J, Rut W. Influence of cofactor binding and active site occupancy on the conformation of macromolecular substrate exosite of factor VIIa, *J. Mol. Biol.* **277**, 959-971, 1998.
61. Wu, Y, Eigenbrot C, Liang W-C, Stawicki S, Shia S, Fan B, Ganesan R, Lipari MT, Kirchhofer D. Structural insight into distinct mechanisms of protease inhibition by antibodies. *Proc. Natl. Acad. Sci. U.S.A.* **104**, 19784-19789, 2007.
62. Farady, CJ, Egea PF, Schneider EL, Darragh MR, Craik CS. Structure of a Fab-protease complex reveals a highly specific non-canonical mechanism of inhibition. *J. Mol. Biol.* **380**, 351-360.
63. Ganesan, R, Eigenbrot C, Wu Y, Liang W-C, Shia S, Lipari MT, Kirchhofer D. Unraveling the allosteric mechanism of serine protease inhibition by an antibody. *Structure.* **17**, 1614-1624, 2009.
64. Schilling, RJ, Mitra AK. Intestinal mucosal transport of insulin. *Int J. Pharm.* **62**, 53-64, 1990.
65. Schilling, RJ, Mitra AK. Degradation of insulin by trypsin and  $\alpha$ -chymotrypsin. *Pharm. Res.* **8**, 721-27, 1991.
66. Lee, VHL, Yamamoto, A. Penetration and enzymatic barriers to peptide and protein absorption. *Adv. Drug Del. Rev.* **4**, 171-207, 1990.
67. Lee, VHL, Dodda-Kashi, S, Grass, GM, Rubas W. Oral route of peptide and protein absorption. In Lee, VHL (Ed.). *Peptide and Protein Drug Delivery*, Dekker, New York, pp. 691-738, 1991.
68. Ikesue, K, Kpeckova, P, Kopecek J. Degradation of proteins by guinea pig intestinal enzymes. *Int. J. Pharm.* **95**, 171-179, 1993.
69. Gibson, SAW, Macfarlane, GT. Studies on the proteolytic activity of *Bacteroides fragilis*. *J. Gen. Microbiol.* **134**, 19-27, 1988.
70. Bai, JPF. Distribution of brush-border membrane peptides along the rat intestine. *Pharm. Res.* **11**, 897-900, 1994.
71. Kopeckova, K, Ikesue K, Kopecek, J. Cleavage of oligopeptide p-nitroanilides attached to N-(2-hydroxy-propyl) methacrylamide copolymers by guinea pig intestinal enzymes. *Makromol. Chem.* **193**, 2605-2619, 1992.

72. Delano FA, Hoyt DB, Schmid-Schönbein GW. Pancreatic Digestive Enzyme Blockade in the Intestine Increases Survival After Experimental Shock. *Shock*. **169**, 1-9, 2013.
73. Rubinstein, A, Tirosh, B. Mucus gel thickness and turnover in the gastrointestinal tract of the rat, responses to cholinergic stimulus and implication for mucoadhesion. *Pharm Res*. **11**, 794-799, 1994.
74. Kopecek, J, Kopeckova, P, Brondsted, H, Rathi, R, Rihova, B, Yeh, P-Y, Ikesue, K. Polymers for colon-specific drug delivery. *J. Control. Release*. **19**, 121-130, 1992.
75. Rihova, B, Rathi, R, Kopeckova P, Kopecek J. In vitro bioadhesion of carbohydrate-containing N-(2-hydroxy-propyl)mehacrylamide copolymers to the GI tract of guinea pigs. *Int. J. Pharm*. **87**, 105-116, 1992.
76. Rubinstein, A, Tirosh, B, Baluom, M, Nassar, T, David, A, Radai, R, Gliko-Kabir, I, Friedman, M. The rationale for peptide drug delivery to the colon and the potential of polymeric carriers as effective tools. *J. Control. Release*. **46**, 59-73, 1997.